Send Orders for Reprints to reprints@benthamscience.net

Current Physical Chemistry, 2014, *4*, 151-172

Prediction of Ionic Liquids Properties through Molecular Dynamics Simulations

Marta L.S. Batista, João A.P. Coutinho and José R.B. Gomes*

CICECO, Departamento de Química, Universidade de Aveiro, 3810-193 Aveiro, Portugal

Abstract: Ionic liquids (ILs) are a new generation of molten salts possessing unique physical and chemical properties, which have gained attention from the academic and industries researchers. The design of new products and processes requires the knowledge of transport and thermophysical properties, yet, due to the large number of potential ILs, their characterization by experimental means alone is not feasible. Computer simulations are being used with success for the prediction of structures and properties of many different molecular systems. Among different computational approaches, molecular dynamics simulation (MD) has proved to be capable of providing a good understanding at the molecular level of how the structure and properties of ILs are related.

This work reviews the literature and presents an outlook of methodologies applied to predict properties of neat ILs, namely, density, viscosity, diffusivity, melting point, enthalpy of vaporization and surface tension. It has been shown that MD simulations are able to reproduce properties of ILs with good enough accuracy for design purposes. However, lack of force field parameters for several different combinations of ILs and lack of accurate experimental data for some properties of ILs, crucial to calibrate the computational procedures, are some problems that still need to be addressed for a better characterization of the chemical and physical properties of ILs by computer simulation.

Keywords: Computer approaches, ionic liquids, molecular dynamics simulations, transport properties, thermophysical properties.

INTRODUCTION

In the early 20th century, a new generation of molten salts was discovered by Paul Walden [1]. These molten salts are nowadays known by different names, such as ionic melts, ionic fluids, or liquid electrolytes but the most common and recognized name is ionic liquids (ILs) [2]. These compounds possess at least one asymmetric unit comprised of a large organic cation, e.g. imidazolium, pyridinium, pyrrolidinium, ammonium or phosphonium, and an organic or inorganic anion, e.g. bis[(trifluoromethyl)sulfonyl]imide, trifluoromethylsulfonate, hexafluorophosphate, or tetrafluoroborate, with structures shown in Fig. (1) [2, 3]. The structural asymmetry makes their crystallization difficult and minimizes the cation-anion interaction conferring unique properties to ILs, *i.e.*, they possess low melting point (<100°C), extremely low vapor pressure, high thermal and chemical stability, high ionic conductivity and good solvating capacity for organic and inorganic compounds and even biopolymers. Furthermore, ILs are nonflammable and are in the liquid state in a wide range of temperatures. Moreover, it is possible to tune their properties by changing the constituting ions, within the wide range of possible combinations of cations and anions, and by adding specific functional groups in order to confer desired physicochemical properties intended for a specific application. Given the possibility of fine-tuning the properties of ILs, their range of applicability is vast. Separation processing, chemical processing, biotechnology, electrochemistry are some of the possible application fields where ILs may act, for example, as solvents, lubricants, electrolytes or heat transfer fluids [2]. Although ILs appeared to be an alternative to replace common solvents, as for example the volatile organic compounds, VOCs, due to their greener character when compared with that of the latter, parameters such as toxicity and biodegradability have lately been of concern in the academic field. Polarity and ionization are other topics of interest and importance which are also discussed [3].

The properties of ILs are influenced by the structural specificities of the cation and of the anion that compose the IL. The knowledge of the structure-property relationships of ILs is required for the selection or design of an IL for a specific application. Thus, knowledge of properties such as densities, viscosities, diffusivities, melting points, vapor pressures, boiling points or dielectric constants of as many ILs as possible is needed. However, the huge number of potential cation/anion combinations makes this task daunting by an experimental approach alone. In an attempt to relate structure with property, group contribution methods and QSPR/QSAR (quantitative structure – property/activity relationships) approaches have been used to predict thermophysical properties, phase behaviors, toxicities, among others, of some ILs [4-7]. A review [8] on these types of methods for the estimation of thermophysical and transport properties of ionic liquids has recently appeared. Also for the same purpose, quantum methods and statistical mechanics-based molecular approaches are gaining, in the past few years, an important role in the field since they have

*Address correspondence to this author at the CICECO, Departamento de Química, Universidade de Aveiro, 3810-193 Aveiro, Portugal;
Tel: +351-234-401423; E-mail: jrgomes@ua.pt

1877-9476/14 $58.00+.00

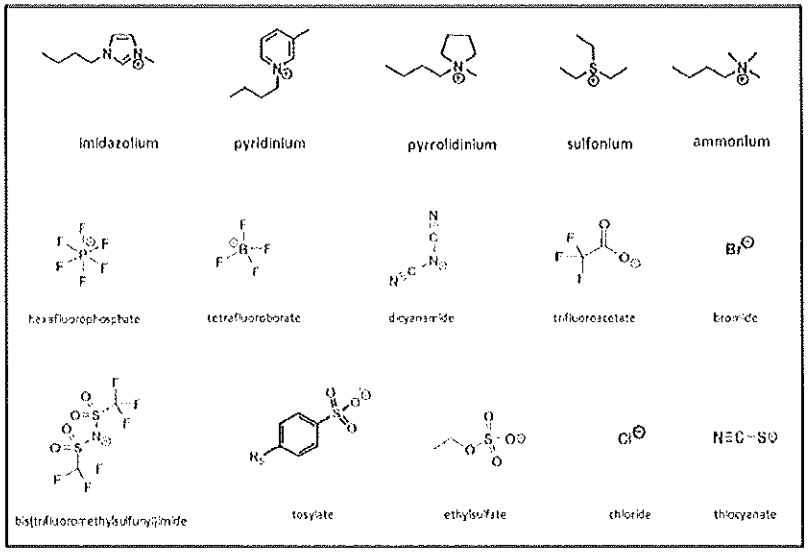

Fig. (1). Most common cations and anions found in literature which compose ionic liquids (ILs).

been helping to better understand, at the molecular level, the structure-property relationships and phase behavior of neat IL and IL in mixtures (with one or more compounds) [9-13]. Inherent to the nature of each moiety is the nature of its self-organization, and the influence on their properties, especially on their behavior as solvents, which is a theme with a growing concern. Canongia-Lopes and co-workers [14-16] are among the pioneering researchers to show that ILs present a structure characterized by two main domains, a polar domain (high-charge density part composed by a hydrophilic head-group) and a non-polar (low-charge density part composed by a hydrophobic tail), at nanometer scale, which have been widely used to justify different behaviors (and properties) of ILs [3]. In a recent work [17], it was possible to conclude that due to this unique structure, ILs present a "chameleonic behavior", a sort of amphiphilic character that allows their simultaneous interaction with two compounds of different polarities. The so-called chameleonic behavior is just an example of how ILs can be complex solvents and, thus, their characterization opened a new and interesting research field.

Given the rather complex molecular structure of ILs, advances at computer simulation have gained a major importance in the field. In this matter, in the past few years, several works including some extended studies or reviews [3, 13, 18-22] have been published concerning the application of computer approaches to model mixtures of ILs and also neat ILs. Ab initio methods, Monte Carlo (MC) and molecular dynamics (MD) simulations, and coarse-grained (CG) simulation methods are computer approaches that are being widely used to model this type of systems at different time and length scales [23-26]. These different approaches are briefly introduced in this review. Furthermore, an overview of methodologies applied to predict properties, namely, density, viscosity, diffusivity, melting point, vapor pressure and boiling point, enthalpy of vaporization and surface tension, is here presented. MD simulation studies employing different computational strategies for calculating physicochemical data of neat ILs and for their characterization are also reviewed.

COMPUTER APPROACHES

There are three main categories of computer approaches able to model and characterize ILs, namely ab initio methods, Monte Carlo and molecular dynamics simulations, and coarse-grained methods [27]. These categories may be distinguished by their capacities to handle different length and time scales, as schematically represented in Fig. (**2**).

The first category comprising the *quantum chemical (QC) methods* is at the *electronic* scale and considers the fundamental particles constituting the atoms, *i.e.*, electrons and nuclei which in the field of ILs translates into the accurate characterization of a single IL molecule (ion pair) or, less accurately, of a small cluster of ILs ions. The electronic structure methods are characterized by requiring large computational efforts due to their full electronic details, which limit their application only to systems composed by a restricted number of atoms (few tens or few hundreds depending on the flavor) and when combining finite temperature dynamics (ab initio molecular dynamics, AIMD [28]), to very short time scales. The electronic structure methods can be divided in methods that formulate the many-electron problem in terms of a many-body wavefunction [27] (Hartree-Fock (HF) approach or the much more accurate - but demanding further computational resources - post-HF methods) or in terms of the electron density [29] (density functional theory, DFT). When high accuracy is required, higher level ab initio approaches (post-HF methods, such as, N-order Moller-Plesset [30, 31], coupled-cluster [32], configuration interaction [33] approaches) are used.

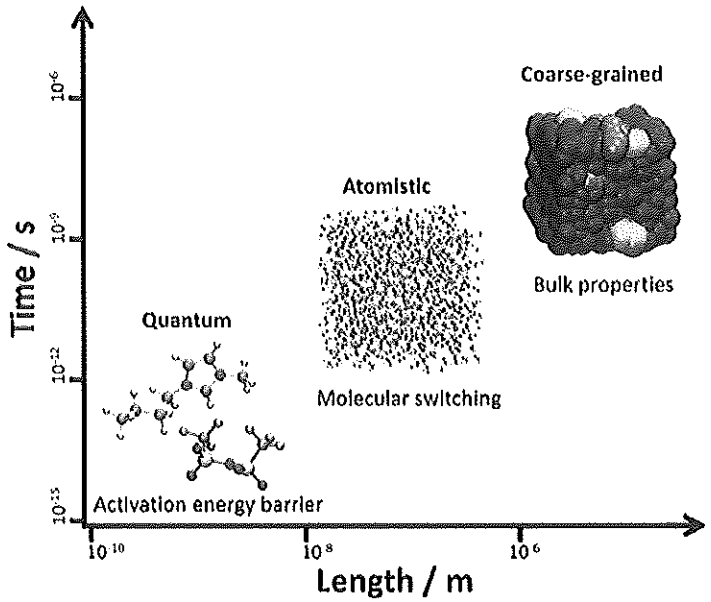

Fig. (2). Illustration of the different length and time scales that can be reached by most common computational approaches.

Nevertheless, these high level methods require large computational efforts limiting their application to rather small systems (a few tens of atoms) and are usually used to refine energies (single-point calculations) [3, 34]. The DFT approaches require less computational resources than post-HF methods without compromising too much the accuracy of the calculations and they are able to deal, chemically speaking, with more interesting molecular systems [3, 34]. Finally, composite methods such as the popular Gaussian-N or Complete Basis Set (CBS) approaches [35] combine the results of several calculations performed at different levels of theory for correction of the deficiencies, *e.g.* incomplete electron correlation or basis set limited size, in the energy of a system optimized with a standard computational approach.

The second category, the atomistic simulations, considers methods at the microscopic level, where the constituting particles in the preceding class are now replaced by atoms (all atom approach) or groups of atoms (united atom approach) that interact through a force field (FF) or intermolecular potential energy, obeying to statistical mechanics.

Since electrons are not being considered in these approaches, the study of chemical reactions (bond making and bond breaking) is not possible. Nevertheless, these approaches are quite appealing since they enable the description of a larger number of constituting atoms than that is possible with QC methods, as well as to simulate longer times of simulation (nanosecond time scale). This kind of simulations usually makes use of periodic boundary conditions (replicas of the central simulation box surrounding it on all sides). This category includes, the widely used Monte Carlo (MC) and Molecular Dynamics (MD) simulation approaches. The MC simulation approach is characterized by being a pure stochastic technique [36], composed by simple algorithms, typically performed on a fixed number of molecules, N, placed on a fixed volume, V, and maintained at a constant absolute temperature T, *i.e.*, the canonical ensemble (NVT). An initial configuration (positions, orientation angles, among others, for the constituting particles) is needed and then an atom (or group of atoms) chosen randomly is moved or rotated by a random amount to another and new configuration. All random configurations are then compiled in a sequence from which equilibrium properties are calculated by average [34, 37, 38]. In the field of ILs, MC simulations have been applied to determine thermodynamic (molar volume, cohesive energy density, isothermal compressibility, cubic expansion coefficient, Henry's law constant, partial molar enthalpy of absorption and solubility in water and CO_2) and structural properties [3, 39-41].

The MD simulation is employed in the study of the natural motion of molecules under the effects of their own intermolecular forces. In the most natural formulation, the simulations are performed for an isolated system (the sum of the molecular kinetic and potential energies yields the total energy, E, which is conserved, *i.e.*, it corresponds to an adiabatic process with no heat exchange) on a fixed number of particles, N, and in a fixed volume, V, *i.e.*, the micro-canonical (NVE) ensemble. Algorithms included in this methodology are more complex and more information is obtained, than those obtained through MC simulations, reproducing motions of individual molecules through the determination of velocities, positions and orientations over time by numerically solving the Newton's equations of motion rather than using a random generator as in Monte Carlo. The forces between the particles and the potential energy of the system are defined by a set of mathematical

functions (force field, FF) with parameters derived from experimental or computational (ab initio) work. The storage of both velocities and positions (large trajectories of systems composed by many particles) in MD requires large amounts of computer memory/disk. From averaging the trajectories, equilibrium and non-equilibrium properties are obtained. In this matter, the MD methods can be divided in two groups, one applied to study systems at equilibrium (equilibrium MD, EMD) and another group to study systems away from equilibrium, (non-equilibrium MD, NEMD), the latter constituting excellent alternatives to EMD for computing transport properties [34, 37, 38].

MC can be more advantageous than MD simulations for discontinuous phenomena, *i.e.*, for systems where molecules interact through discontinuous forces (*i.e.*, perturbation/ changes that a system can suffer such a slow phase transition, micelle formation or polymer folding) though Liu and co-workers [42] showed that MD can also be used for that purpose. Nevertheless, MD simulations stand out due to their ability to describe dynamical behavior and transport properties, *e.g.*, diffusive, convective and other motion phenomena at molecular level [34, 37, 38].

It is important to add that MD simulations can also be formulated for ensembles other than the microcanonical one, but it is imperative to make sure that the correct dynamic trajectories are preserved. For that, thermostats and barostats can be attached to the system for controlling temperature and pressure, respectively. For temperature the simplest method is to rescale velocities at periodic intervals such that a desired temperature is maintained. However, this does not obey Maxwell-Boltzmann distribution (the equilibrium distribution of velocities) and improvements have been made, such as the Andersen [43] and the Nosé-Hoover [44] thermostats. For barostats, the same limitation is observed, and an extension of Nosé-Hoover thermostat [45] can be used as barostat by using volume fluctuations. Other barostats such as the Berendsen [46] or Parrinello-Rahman [47, 48] also exist (again the main difference is that the latter can, in theory, give a true NPT ensemble). The influence of employing different barostats and thermostats in the trajectories, however, is not relevant when the purpose is to obtain static and thermodynamic properties, as long as they are able to produce the correct canonical ensemble distribution (NVT), or the correct isothermal-isobaric ensemble (NPT) [34].

Standard MD simulations as well as MC simulations are performed with fixed charges (this is a topic that has been strongly discussed in the past years) [3, 49-53] which have a strong influence in the quality and accuracy of the results coming from the calculations. Variations in charge distribution with dielectric environment can be taken into account with the so-called polarizable force fields, which are more accurate (*e.g.* water) but more computational demanding. Thus, the choice of the force field for a specific simulation on a specific system is very important: standard CHARMM (Chemistry at HARvard Molecular Mechanics) [54], OPLS-UA (Optimized Potential for Liquid Simulations - United Atoms) [55], OPLS-AA (Optimized Potential for Liquid Simulations - All Atoms) [56] and AMBER (Assisted Model Building and Energy Refinement) [57] are some of the existing FFs commonly used for ILs. However, the force fields were originally optimized to reproduce the properties of liquids or to handle biomolecular systems and, hence, their parameters have to be adjusted for ILs. Moreover, the question of transferability of parameters from one force field to another is a very important issue [58].

The speed of computers can also be limiting, especially for what concerns the simulation time that is needed to reproduce the properties of the systems of interest accurately. In all atom (or even united atom) MD simulations, due to these time limitations, very large systems and slow phenomena are beyond the length and time scales permitted. Still, in the field of ILs, MD presents enormous advantages over other computationally more expensive approaches (ab initio methods) providing reliable structural, thermodynamic and transport properties [3].

The third and last category involves *mesoscale* methods, such as lattice models and the coarse-grained (CG) approach. The latter considers particles that are used to represent molecules, segments of molecules or even clusters of molecules, and also discretization of phase space and representation of the system in terms of fields, rather than the description of every atom in the system. In other words, the representation of molecules or groups of small molecules is now made by a small number of large particles, reducing the degrees of freedom and the number of pair interactions and hence, the computational efforts required for the simulation of a specific system [35, 59]. Thus, with the CG approach, it is possible to increase the number of particles that can be simulated and/or to increase the time scale of the simulations. This can be very convenient in the study of large molecules such as polymers (proteins, carbohydrates) or ILs with long side chains (butyl, heptyl or decyl), increasing the time scale and the number of particles that can be simulated, or even in the simulation of slow phenomena such as sphere to rod transitions of surfactant micelles [3, 35, 59-61]. The price that has to be paid is that the local information is lost. In fact, the contribution of atom vibrations is removed as well as the internal degrees of freedom, which promotes a simulation to occur rather faster than the real one, losing the true dynamics of the system in study. Due to these limitations, multiscale modeling is usually useful, in the sense that the information obtained from CG simulations may be used *a posteriori* in MC or MD simulations (combination of information obtained from different level scales) [34, 59]. Recently, Chen and co-workers [62] reviewed different coarse-grained models and highlighted differences, applications and limitations of these computational methodologies.

PREDICTION OF ILS PROPERTIES THROUGH MD SIMULATIONS

In the forthcoming sub-sections, some properties used to characterize ILs are introduced and pertinent reference to reported MD simulation studies for neat ILs, aiming at their determination, will be given. Some computational details concerning the MD simulation works reviewed here are compiled in Table 1.

Density

This is one of the most important properties of fluids that is easily measured experimentally and is fundamental for the

Table 1. Detailed information concerning the MD simulations of reported studies in this article.

Author(s)	Ionic Liquid	Pairs[a]	Charges, Value[b,c]	Potential[c]	Ref.
Alavi and co-workers	[patr][Br]	144	NPA, ± 1e	AMBER & OPLS-AA & GAFF	[90]
Alavi and Thompson	$[C_2C_1im][PF_6]$	192	CHelpG , ± 1e	AMBER & OPLS-AA	[89]
Aparicio and co-workers	$[C_2C_1im][TOS]$	250	ESP, ± 1e	OPLS-AA	[114]
Batista and co-workers	$[C_4C_1im][NTf_2]$	200	CHelpG , ± 0.797e	C: CHARMM ; A: OPLS-AA / Gromos	[68]
	$[C_4C_1im][SCN]$	200	CHelpG , ± 0.804e		
Bhargava and Balasubramanian	$[C_4C_1im][PF_6]$	256	CHelpG , ± 0.80e	AMBER & OPLS-AA	[49]
Borodin	$[C_2C_1im][NTf_2]$	125-180		polarizable	[106]
	$[C_4C_1im][NTf_2]$				
	$[C_6C_1im][NTf_2]$				
	$[C_4C_1im][PF_6]$				
	$[C_4C_1im][BF_4]$				
	$[C_4C_1im][CF_3SO_3]$				
	$[N_{4111}][NTf_2]$				
	$[pyr_{14}][NTf_2]$				
Brandés and co-workers	$[C_2py][BF_4]$	125	ESP, ± 1e	OPLS-AA	[74]
	$[C_4C_1py][BF_4]$				
Canongia Lopes and co-workers	$[C_1C_1im][Cl]$	192	CHelpG , ± 1e	AMBER & OPLS-AA	[24]
	$[C_2C_1im][Cl]$	144			
	$[C_2C_1im][NO_3]$	96			
	$[C_2C_1im][PF_6]$	192			
Canongia Lopes and Pádua	$[C_4py][Cl]$	144	CHelpG , ± 1e	OPLS-AA	[123]
	$[P_{10\,10\,10\,10}][Br]$	16			
	$[N_{1\,1\,1\,1}][N(CN)_2]$	96			
Chaban	$[C_1C_1im][NTf_2]$	128	uniform scaling charges	AMBER & OPLS-AA	[125]
Ghatee and co-workers	$[C_4C_1im][I]$	512	CHelpG, scaled charges	OPLS-AA	[75]
	$[C_6C_1im][I]$				
	$[C_8C_1im][I]$				
Heggen and co-workers	$[C_4C_1im][PF_6]$	512	CHelpG , ± 0.80e	AMBER & OPLS-AA	[117]
Jayaraman and Maginn	$[C_4C_1im][Cl]$	144	CHelpG , ± 1e	OPLS-AA CHARMM	[94]
Kelkar and co-workers	$[C_2C_1im][NTf_2]$	200	CHelpG , ± 1e	CHARMM	[104]
	$[C_4C_1im][NTf_2]$				
	$[C_6C_1im][NTf_2]$				
	$[C_8C_1im][NTf_2]$				
Klähn and co-workers	AP-N[d]	500	CHelpG , ± 1e	Molecular Mechanics (MM)	[107]
	AP-C[e]				
	CM-N[f]				

Table 1. contd....

Author(s)	Ionic Liquid	Pairs[a]	Charges, Value[b,c]	Potential[c]	Ref.
Koddermann and co-workers	$[C_2C_1im][NTf_2]$	173	CHelpG , ± 1*e*	AMBER & OPLS-AA	[105]
	$[C_4C_1im][NTf_2]$				
	$[C_6C_1im][NTf_2]$				
	$[C_8C_1im][NTf_2]$				
Liu and co-workers	$[C_4C_1im][Pf_2]$	200	RESP , ± 0.80*e*	GAFF	[73]
	$[C_3C_1pyr][NTf_2]$				
	$[N_{4111}][NTf_2]$				
Margulis and co-workers	$[C_4C_1im][PF_6]$	256	ESP, ± 1*e*	OPLS-AA	[66]
Pensado and co-workers	$[C_2C_1im][BF_4]$	1024	CHelpG , ± 1*e*	AMBER & OPLS-AA	[121]
	$[C_2OHC_1im][BF_4]$	700			
	$[C_8C_1im][BF_4]$	700			
	$[C_8OHC_1im][BF_4]$	800			
Prado and co-workers	$[C_4C_1im][BF_4]$	125	CHelpG , ± 1*e*	OPLS-AA	[67]
Santos and co-workers	$[C_2C_1im][NTf_2]$	400	CHelpG , ± 1*e*	AMBER/OPLS	[103]
	$[C_4C_1im][NTf_2]$				
	$[C_6C_1im][NTf_2]$				
	$[C_8C_1im][NTf_2]$				
Shimizu and co-workers	$[C_2C_1im][NTf_2]$	150	CHelpG , ± 1*e*	AMBER/OPLS - AA	[76]
	$[C_4C_1im][NTf_2]$				
	$[C_6C_1im][NTf_2]$				
	$[C_8C_1im][NTf_2]$				
	$[C_{10}C_1im][NTf_2]$				
	$[C_{12}C_1im][NTf_2]$				
	$[C_{14}C_1im][NTf_2]$				
	$[C_4C_1im][PF_6]$				
	$[C_6C_1im][PF_6]$				
	$[C_8C_1im][PF_6]$				
	$[P_{6,6,6,14}][NTf_2]$				
	$[P_{6,6,6,14}][CF_3SO_3]$				
	$[P_{6,6,6,14}][OAc]$				
	$[C_4C_1im][CF_3SO_3]$				
	$[C_4C_1im][CH_3SO_4]$				
	$[C_4C_1im][BF_4]$				
	$[C_4C_1im][OAc]$				
Shimizu and co-workers	$[PH(C_6H_5)_3][N(SO_2F)_2]$	144	CHelpG , ± 1*e*	OPLS-AA	[124]
	$[Na][N(SO_2C_2F_5)_2]$	96			
	$[K][N(SO_2C_2F_5)_2]$	128			
	$[(OCH_3)_2C_1im][PF_3(C_2F_5)_3]$	144			

Table 1. contd....

Author(s)	Ionic Liquid	Pairs[a]	Charges, Value[b,c]	Potential[c]	Ref.
Van-Oanh and co-workers	$[C_2C_1im][NTf_2]$	50 and 150	CHelpG, ± 1e	C:CHARMM & A: OPLS-AA	[112]
Yan and co-workers	$[C_4C_1im][NO_3]$	400	RESP, ± 1e	non-polarizable polarizable	[83]
Zhang and Maginn	$[C_4C_1im][Cl]$	108	CHelpG, ± 1e	C: CHARMM ; A: OPLS	[95]
Zhang and Maginn	$[C_4C_1im][PF_6]$	250	gpFC, ±1e	CHARMM	[77]
			gpSC, ± 0.80e		
			AIMD-c, ± 0.80e		
			AIMD-l, ± 0.85e		
			AIMD-b, ± 0.80e		
	$[C_2C_1im][PF_6]$	400	gpFC, ±1e		
			gpSC, ± 0.80e		
			AIMD-c, ± 0.80e		
			AIMD-l, ± 0.85e		
			AIMD-b, ± 0.76e		
Zhao and co-workers	$[C_4C_1im][PF_6]$	768	CHelpG, ± 0.80e	OPLS-AA	[113]
Zhong and co-workers	$[C_1C_1im][NTf_2]$	150	RESP, ± 0.80e	GAFF	[72]
	$[C_2C_1im][NTf_2]$				
	$[C_6C_1im][NTf_2]$				
	$[C_8C_1im][NTf_2]$				
	$[C_4C_1im][CF_3CO_2]$				
	$[C_4C_1im][CH_3CO_2]$				
	$[C_4C_1im][PF_6]$				
	$[C_4C_1im][NTf_2]$				

[a]Number of cation+anion pairs in the simulation box;
[b]ESP, RESP and CHelpG are charges based on the fitting of the electrostatic potential on a grid of points according to the schemes of Merz-Singh-Kollman [78, 80-81] or of Bayly and co-workers [82], respectively. NPA and Blöchl stand for charges derived from a natural population analysis of the natural bond orbitals approach of the atoms in a molecular system [129] or for charges calculated using the Blöchl method [79]. The labels gpFC and gpSC are used to denote full and scaled RESP charges for the isolated ions in the gas-phase calculated with Gaussian-type orbitals, AIMD-c is used for ESP charges calculated for the crystalline system using a plane-wave approach while AIMD-l and AIMD-b stand for charges calculated after liquid phase simulations employing a plane-wave approach and the ESP or the Blöchl schemes, respectively.
[c]C and A stand for cation and for anion, respectively;
[d]acyclic pentamethylpropylguanidinium nitrate;
[e]acyclic pentamethylpropylguanidinium perchlorate;
[f]cyclic tetramethylguanidinium nitrate.

prediction of thermophysical properties required for process design purposes or for solution theories of liquids. For ambient pressure and temperature conditions, the density of common ILs range from 0.9 to 1.5 $g \cdot cm^{-3}$ [63]. Available data for ILs density, in literature, is impressive and it is well reproduced by MD simulations [19, 64, 65]. In Maginn's review [19] on the application of atomistic simulations to the prediction of thermodynamic and transport properties of ILs, computed and experimental densities were found to differ at most by 1% to 5%, depending on the applied force field and on its parameterization. Density is essentially a mean-field property that is insensitive to specific interactions and energies; yet, it is one of the properties that is widely used to validate force fields due to the two factors introduced above, *i.e.*, simplicity of calculation and availability of very accurate experimental values [13].

Densities of several different ILs were studied by means of MD simulations. Margulis and co-workers [66] conducted MD simulations considering the OPLS-AA (optimized potentials for liquid simulations developed by Jorgensen and co-workers [56] combined with an all atoms approach and total charges on the ions equal to unity) force field for at least 200 ps in the NPT ensemble, *i.e.*, constant pressure (1 atm, Nosé Hoover thermostat) and constant temperature (303 K, Anderson-Hoover barostat), for 1-butyl-3-methylimidazolium hexafluorophosphate ($[C_4C_1im][PF_6]$), obtaining a density with the value of 1310.0 kg/m^3; Zhong

and co-workers considered a different FF and different total charges on the ions (± 0.8*e*) and reached a density value for the same IL that matches the experimental result, *i.e.*, 1370.0 kg/m^3 (Table **2**). Prado and co-workers [67] using the OPLS-AA force field and charges equal to unity performed simulations for at least 5 ns and reached a density value of 1178.0 kg/m^3 for 1-butyl-3-methylimidazolium tetrafluoroborate, $[C_4C_1im][BF_4]$, also very close to the experimental result (c.f. Table **2**). In these MD simulations, it was found that the density is converged for quite short simulation times. Batista and co-workers [68], estimated the density of 1-alkyl-3-methylimidazolium bis(trifluoromethylsulfonyl)imide ($[C_4C_1im][NTf_2]$) and 1-alkyl-3-methylimidazolium thiocyanate ($[C_4C_1im][SCN]$), using potential parameters taken from published works [11, 69, 70] or derived from the Gromos force field but with recalculated atomic charges (different from unity). They obtained density values of 1486.0 and of 1082.0 kg/m^3 for $[C_4C_1im][NTf_2]$ and for $[C_4C_1im][SCN]$, respectively, also in good agreement with experimental data. Recently, densities of a series of different ILs, 1-alkyl-3-methylimidazolium bis(trifluoromethylsulfonyl)imide ($[C_nC_1im][NTf_2]$) and 1-butyl-3-methylimidazolium cation ($[C_4C_1im]^+$) with different anions, such as, trifluoroacetate ($[CF_3CO_2]^-$), acetate ($[CH_3CO_2]^-$) or hexafluorophosphate($[PF_6]^-$), were obtained at different temperatures through NPT MD simulations and considering the General Amber Force Field, GAFF [71] , by Zhong and co-workers [72]. The deviation of the results from experimental data (cited in the article) is less than 1%. In that work, a linear behavior of the density with the temperature was observed for all studied ILs. Furthermore, as expected, the densities of different alkyl chain lengths of imidazolium based-ILs with the anion $[NTf_2]^-$, decreased with the increase of temperature. Similarly, Liu and co-workers [73] published a complete study, estimating density for $[NTf_2]^-$-based ILs, obtaining a linear and a decreasing dependence with the increase of the temperature. The comparison of their results with published experimental data was found to be good. For two other families of ILs, namely, pyridinium-based ILs and iodide-based ILs studied by Bandrés and co-workers [74] (with a maximum deviation of 14% from experimental data) and by Ghatee and co-workers [75] (with a maximum deviation of 0.8% from experimental data), respectively, a similar trend with the temperature was observed. Shimizu and co-workers [76], reported densities for imidazolium-based ILs and for some phosphonium-based ILs, with deviations not exceeding 4.5 %.

Densities of 1-ethyl-3-methylimidazolium hexafluorphosphate, $[C_2C_1im][PF_6]$, and 1-*N*-butyl-3-methylimidazolium hexafluorphosphate, $[C_4C_1im][PF_6]$, were obtained at 173 K through NVT and NPT MD simulations, considering GAFF force field, by Zhang and Maginn [77]. These authors evaluated the influence of five different strategies for the calculation of atomic charges, which were incorporated in the general Amber force field, on the prediction of static, dynamic and thermodynamic properties of $[C_4C_1im][PF_6]$ and $[C_2C_1im][PF_6]$ ILs by MD simulation. They tested the influence of atomic charges derived from periodic DFT/plane-wave calculations, for the crystalline and liquid phases, or from quantum chemistry calculations for the isolated ions. In the case of the periodic crystalline phase, the total charges calculated with the ESP scheme [78] were ± 0.80*e* on the cation and on the two anions considered, respectively. The ESP charges were calculated by fitting the electrostatic potential of a molecule on a uniform distribution of points in the vicinity of the molecule. In the case of liquid phase, the calculation of the atomic charges was based on 50 different configurations taken from an AIMD simulation with 8 IL pairs per unit cell and considering two different schemes, *i.e.*, the Blöchl [79] and the ESP [78, 80-82] schemes. The Blöchl method decouples the density of a molecule calculated with a periodic plane-wave approach from its periodic images, *i.e.*, by subtracting the electrostatic interaction between periodic images of the densities of the isolated molecules. The interaction energy between separated densities is expressed in electrostatic multipole moments which reproduce the original density and are used to fit the partial charges. The total charges in the cation and in the anion calculated with the ESP scheme were ± 0.85*e* for both ILs while those calculated with the Blöchl scheme were ± 0.80*e* for $[C_4C_1im][PF6]$ and ± 0.76*e* for $[C_2C_1im][PF6]$, *c.f.* Table **1**. Finally, Zhang and Maginn considered also full atomic charges derived from quantum chemistry calculation of isolated ions in vacuum (total charge ± 1.0*e* for each ion), and charges derived from uniform scaling by a factor of 0.8 of the charges of the isolated ions in vacuum. As can be seen in Table **2**, the densities calculated with the five different sets of charges resulted in similar density values which have a maximum deviation of 6% from available experimental data. Thus, it seems that the value of the total charge in the cation and in the anion of ILs and the strategy used for the calculation of the atomic charges have a small effect on the calculation of this property.

Due to the fact that density is a validation parameter of force fields, almost all the MD computational studies in this field present density data which is compared with experimental results or with other published computational data. Nevertheless, and as it was mentioned previously, density is insensitive to specific interactions and energies, and issues such as the polarization of the force field is practically not applicable, since polarizable and non-polarizable force fields reproduce results in good agreement with experimental ones (see Table **2**) [58]. A similar conclusion was reached by Yan and co-workers [83], who, in an evaluation of the main differences in the application of polarizable and non-polarizable force fields in the estimation of properties of 1-ethyl-3-methylimidazolium nitrate, $[C_2C_1im][NO_3]$, obtained the values of 1177 kg/m^3 and 1174 kg/m^3 from simulations employing polarizable and non-polarizable force fields, respectively. These findings are in agreement with the results due to Zhang and Maginn [77] where total charges in the ions of two ILs ranging from ± 0.76*e* to ± 1.0*e* yielded practically the same densities and show that this property is quite insensitive to the values of the charges considered in the simulations.

Melting Point

As mentioned previously, a large and asymmetric cation together with an (in)organic anion confers to the IL a specific structure that prevents its crystallization, and thus

Table 2. Estimated densities by means of MD simulations and experimental data, at different temperatures.

Author(s)	Ionic Liquid	T / K	ρ_{sim} / kg.m^{-3}	ρ_{exp} / kg.m^{-3}
Batista and co-workers	$[C_2C_1im][NTf_2]$	298	1486	1437.0 [129]
	$[C_4C_1im][SCN]$		1082	1069.8 [130]
Ghatee and co-workers	$[C_4C_1im][I]$	323	1.414	1418
	$[C_6C_1im][I]$		1.313	1318
	$[C_8C_1im][I]$		1.248	1240
Liu and co-workers	$[C_4C_1im][NTf_2]$	298	1446	1437.0 [129]
	$[C_4C_1im][PF_6]$		1523	1517.7
	$[C_4C_1pyr][NTf_2]$		1439	1406.1
	$[N_{4111}][NTf_2]$		1493	1398.4
Margulis and co-workers	$[C_4C_1im][PF_6]$	298	1310	1370.0 [131]
Prado and co-workers	$[C_4C_1im][BF_4]$	298	1178	1170
Shimizu and co-workers	$[C_2C_1im][NTf_2]$	298	1.6	1.5
	$[C_4C_1im][NTf_2]$		1.5	1.4
	$[C_6C_1im][NTf_2]$		1.4	1.4
	$[C_8C_1im][NTf_2]$		1.4	1.3
	$[C_{10}C_1im][NTf_2]$		1.3	1.3
	$[C_{12}C_1im][NTf_2]$		1.3	1.2
	$[C_{14}C_1im][NTf_2]$		1.2	1.2
	$[C_4C_1im][PF_6]$		1.3	1.4
	$[C_8C_1im][PF_6]$		1.3	1.3
	$[C_8C_1im][PF_6]$		1.2	1.2
	$[P_{6,6,6,14}][NTf_2]$		1.1	1.1
	$[P_{6,6,6,14}][CF_3SO_3]$		1	1
	$[P_{6,6,6,14}][OAc]$		0.9	0.9
	$[C_4C_1im][CF_3SO_3]$		1.3	1.3
	$[C_4C_1im][CH_3SO_4]$		1.2	1.2
	$[C_4C_1im][BF_4]$		1.2	1.2
	$[C_4C_1im][OAc]$		1.1	1.1
Zhang and Maginn	$[C_4C_1im][PF_6]$	173	1484[a]	1560
			1461[b]	
			1475[c]	
			1479[d]	
			1471[e]	
	$[C_2C_1im][PF_6]$		1615[a]	1656
			1578[b]	
			1593[c]	
			1599[d]	
			1577[e]	

Table 2. contd....

Author(s)	Ionic Liquid	T / K	ρ_{sim} / kg.m^{-3}	ρ_{exp} / kg.m^{-3}
Zhong and co-workers	$[C_4C_1im][PF_6]$	298	1370	1370.0 [131]
	$[C_4C_1im][NTf_2]$		1445	1437.0 [129]
	$[C_1C_1im][NTf_2]$		1578	1570.0 [132]
	$[C_2C_1im][NTf_2]$		1531	1519.2
	$[C_6C_1im][NTf_2]$		1375	1371.0 [133]
	$[C_5C_1im][NTf_2]$		1324	1325.0 [129]
	$[C_4C_1im][CF_3CO_2]$		1212	1210.0 [134]
	$[C_4C_1im][CH_3CO_2]$		1055	1019.2 [135]

[a]gpFC; [b]gpSC; [c]AIMD-c; [d]AIMD-1; [e]AIMD-b charges defined in footnotes of Table 1.

decreases its melting point. This is one of the main differences between common molten salts and ILs, which also allow ILs to be used as replacements of common solvents, and thus, applied in a vast range of applications.

From experimental data [84, 85] it is known that melting points of ILs are influenced by changes in the symmetry between cation and anion, flexibility in the chains of the anions and charge dispersion, which decreases the melting points. However, an increase in the length of the alkyl chains of the cations (increasing the dispersive interactions) will increase the melting point [64, 86].

For the estimation of melting points, through atomistic methods, two approaches can be distinguished, the "direct" and the free-energy based methods. The first group includes solid-liquid interface [87] methods, the hysteresis method [88] (the most common) and the void method [89, 90]. In an attempt to reproduce experimental measurements, Alavi and Thompson [89, 90] used the first method considering constant temperature and pressure MD simulations, to estimate melting points for 1-ethyl-3-methylimidazolium hexafluorophosphate ($[C_2C_1im][PF_6]$) and for 1-n-butyl-4-amino-1,2,4-trizolium bromide([patr][Br]). These simulations were made for the crystal phase at increasing temperature until a melting transition, identified by an abrupt change in density, was observed. However, these melting transitions may occur at higher temperatures than the true melting point, and hence, cannot be detected in the time scales accessible by MD. To overcome this, the void induced melting method systematically introduces voids in the crystal, removing atoms or ion pairs from the lattice. At void densities between 6% and 10%, the apparent melting points level off and this value is taken as the true melting point. Above 10%, the crystal becomes mechanically unstable and results may be unreliable.

Melting point can be thermodynamically defined as the temperature at which the free energy of the liquid becomes equal to that of the solid, and this is the basis for the second group, the free-energy based methods. From the first free-energy based methods [91-93], Jayaraman and Maginn [94] developed a new simulation method, an extension of pseudo-supercritical path (PSPC) sampling procedure, to estimate melting points without the knowledge of fluid and solid reference state absolute free energies (Equation 1).

$$\frac{G}{RT} - \left(\frac{G}{RT}\right)_{ref} = \int_{T_{ref}}^{T} -\frac{H}{RT^2} dT \qquad (1)$$

This procedure is detailed in the literature [94], taking the 1-*n*-butyl-3-methylimidazolium chloride IL ($[C_4C_1im][Cl]$) as a case study for which melting points were estimated for two crystal polymorphs. The calculated results are in good agreement with experimental results from Holbrey and co-workers [85]. Recently, Zhang and Maginn [95] published an extended study on different methods that can be used to calculate melting points. By considering potential parameters derived from the CHARMM force field, they estimated the melting point for the $[C_4C_1im][Cl]$ IL through three different methods, *e.g.*, interface, voids and pseudosupercritical path (PSCP) methods (Table 3). The former method, as mentioned before should present a transition in density (or volume), and in this specific IL it was only possible to detect a sharp increase in the density in a range between 450 and 500 K. In the case of the second method, three transition steps were observed, being impossible to determine the effective melting point. The PSCP method yielded the best result, *i.e.*, it was possible to calculate the melting point for a temperature of 320 K, and therefore it seems to be a reliable approach for the determination of melting point of complex molecules, such as ILs. The same authors in a subsequent work estimated melting points for $[C_2C_1im][PF_6]$ and $[C_4C_1im][PF_6]$, through NVT and NPT MD simulations considering GAFF force field and different methodologies to estimate the atomic charges (c.f previous section and Table 1) [77]. As shown in Table 3, the melting points calculated with the PSCP method, but using different total/atomic charges, are found to differ by 63 K in the case of $[C_4C_1im][PF_6]$ and by 93 K in the case of $[C_4C_1im][PF_6]$ IL. Taking these two ILs, the best agreement between computed and experimental melting points is obtained with the charges calculated from the periodic crystalline phase plane-wave calculations, *i.e.*, AIMD-c charges. These results show that, contrary to what was found for the density, the strategy used to compute the atomic point charges has an important influence in the quality of the calculated melting points.

Table 3. Comparison of estimated melting points obtained using different methodologies and MD simulations, $T_{m,sim}$, with available experimental, $T_{m,exp}$, data.

Author(s)	Ionic Liquid	Method	$T_{m,sim}$ / K	$T_{m,exp}$ / K
Zhang and co-workers	$[C_1C_1im][Cl]$	Interface	450~500	341.95 [136]
		Voids	not possible to identify	
		PSCP	320	
Zhang and Maginn	$[C_1C_1im][PF_6]$	PSCP	292 [a]	284 [137]
			245 [b]	
			284 [c]	
			260 [d]	
			308 [e]	
	$[C_2C_1im][PF_6]$	PSCP	382 [a]	338 [138]
			297 [b]	
			330 [c]	
			332 [d]	
			289 [e]	

[a]gpFC; [b]gpSC; [c]AIMD-c; [d]AIMD-1; [e]AIMD-b charges defined in footnotes of Table 1.

Vapor Pressure, Boiling Point and Enthalpy of Vaporization

The volatility of ILs had been initially considered to be negligible [96]. ILs were regarded as having no measurable vapor pressure and not able to be distilled. However, Earle and co-workers [97] showed that ILs could be distilled under specific temperature and pressure conditions. Later, Rebelo [98] and Paulechka [99] and their co-workers have fully explored the volatility of ILs by demonstrating the potential for vaporizing certain ILs at reduced pressure. These findings paved the way for the measurement of vapor pressures for ionic liquids, mainly by Knudsen effusion methods [99, 100]. The experimental measurement of the vapor pressure and the enthalpy of vaporization was found to be extremely difficult due to the very low vapor pressures and to the competition between vaporization and thermal decomposition (preventing the measurement of critical properties) or to the presence of impurities [64, 72, 86]. In a recent review by Esperança and co-workers [96], the nature of the vapor phase was discussed and the approaches used to predict and measure boiling points, vapor pressures and enthalpies of vaporization of ILs were analyzed. That work highlights the difficulties in the measurement of these properties, and that the accuracy of those data is essential for theoretical and practical purposes.

In simulation, enthalpy of vaporization (ΔH^{vap}) is calculated from the difference between the molar internal energy of the gas (U^{gas}) and of the liquid (U^{liq}) phases (Equation 2).

$$\Delta H^{vap} = RT - \left(U^{liq} - U^{gas}\right) \quad (2)$$

$$\Delta H^{vap} = U^{cohesive} + RT \quad (3)$$

The gas phase is simulated by an isolated ion pair of ILs at the same temperature as the liquid phase [101, 102]. Though the review of Esperança and co-workers [96] does the survey of MD simulations in the prediction of the enthalpies of vaporization of ILs, it can be highlighted some computational works devoted to the estimation of this property. Santos and co-workers [103], estimated enthalpies of vaporization of 1-alkyl-3-methylimidazolium bis (trifluoromethylsulfonyl)imide ($[C_nC_1im][NTf_2]$) according to Eq. 2, based on the force field developed by Canongia-Lopes, Deschamps and Pádua [24]. The same ILs were studied by Kelkar and Maginn [104], but considering a force field based on CHARMM parameters. The values calculated by these authors are compared in Table 4 with those obtained in a indirect way by Shimizu and co-workers [76] and by Köddermann and co-workers [105] from the estimation of the cohesive energy ($U^{cohesive}$) and from the consideration of Eq. 3. As it can be seen in Table 4, different force field parameters and/or different strategies to calculate the enthalpy of vaporization lead to enthalpic differences that can be of several tens of kJ/mol, being the values calculated by Koddermann and co-workers systematically smaller than the experimental results and than those calculated by the other research groups. In fact, the computational results from these four independent studies differ significantly from the experimental results. More recently, several different authors performed computational studies for this family of ILs and their calculated enthalpies of vaporization, obtained with different sets of computational parameters, are closer to the values of Koddermann and co-workers than to those from the other authors listed above. Batista and co-workers [68], considering the same methodology as Santos and co-workers [103], but charges of approximately $\pm 0.8e$, calculated an enthalpy of vaporization for $[C_4C_1im][NTf_2]$ of ~132 kJ/mol.

Table 4. Calculated and experimental enthalpies of vaporization, at T=298 K, for several ILs.

Author(s)	Ionic Liquid	ΔH°_{vap} / (kJ/mol)	ΔH°_{exp} / (kJ/mol)
Batista and co-workers	$[C_4C_1im][NTf_2]$	131.7	134-155 [96, 103, 139]
	$[C_4C_1im][SCN]$	123	148 [139]
Brandés and co-workers	$[C_4py][BF_4]$	190.6	167 [139]
	$[C_4C_1py][BF_4]$	180.5	162.1 [140]
Borodin	$[C_4C_1im][PF_6]$	150.6	157.0 [141]
	$[C_4C_1im][CF_3SO_3]$	142.7	
	$[C_4C_1im][BF_4]$	140.8	
	$[C_2C_1im][NTf_2]$	127.7	134-141 [96, 103, 139]
	$[C_4C_1im][NTf_2]$	133.7	134-155 [96, 103, 137]
	$[C_6C_1im][NTf_2]$	141.9	139 [139], 173 [103]
Kelkar and co-workers	$[C_2C_1im][NTf_2]$	146	134-141 [96, 103, 139]
	$[C_4C_1im][NTf_2]$	151	134-155 [96, 103, 139]
	$[C_6C_1im][NTf_2]$	157	139 [139], 173 [103]
	$[C_8C_1im][NTf_2]$	162	149 [139], 192 [103]
Klähn and co-workers	AP-N	174.5	201.4
	AP-C	189.2	192.4
	CM-N	200.8	218.4
Koddermann and co-workers	$[C_2C_1im][NTf_2]$	130.6	134-141 [96, 103, 139]
	$[C_4C_1im][NTf_2]$	135.1	134-155 [96, 103, 139]
	$[C_6C_1im][NTf_2]$	143.8	139 [139], 173 [103]
	$[C_8C_1im][NTf_2]$	153.8	149 [139], 192 [103]
Santos and co-workers	$[C_2C_1im][NTf_2]$	159	134-141 [96, 103, 139]
	$[C_4C_1im][NTf_2]$	174	134-155 [96, 103, 139]
	$[C_6C_1im][NTf_2]$	184	139 [139], 173 [103]
	$[C_8C_1im][NTf_2]$	201	149 [139], 192 [103]
Shimizu and co-workers	$[C_2C_1im][NTf_2]$	173.47	134-141 [96, 103, 139]
	$[C_4C_1im][NTf_2]$	180.47	134-155 [96, 103, 139]
	$[C_6C_1im][NTf_2]$	185.47	139 [139], 173 [103]
	$[C_8C_1im][NTf_2]$	189.47	149 [139], 192 [103]
	$[C_{16}C_1im][NTf_2]$	199.47	
	$[C_{12}C_1im][NTf_2]$	207.47	
	$[C_{14}C_1im][NTf_2]$	217.47	
	$[C_4C_1im][PF_6]$	186.47	157.0 [141]
	$[C_6C_1im][PF_6]$	194.47	
	$[C_8C_1im][PF_6]$	202.47	169 [139]
	$[P_{6,6,6,14}][NTf_2]$	269.47	
	$[P_{6,6,6,12}][CF_3SO_3]$	258.47	
	$[P_{6,6,6,14}][OAc]$	282.47	
	$[C_4C_1im][CF_3SO_3]$	181.47	
	$[C_4C_1im][CH_3SO_4]$	201.47	
	$[C_4C_1im][BF_4]$	182.47	
	$[C_4C_1im][OAc]$	281.47	

Table 4. contd....

Author(s)	Ionic Liquid	ΔH^{vap}_{sim} / (kJ/mol)	ΔH^{vap}_{exp} / (kJ/mol)
Zhang and Maginn	$[C_2C_1im][PF_6]$	188.2[a]	157.0 [141]
		145.1[b]	
		143.0[c]	
		144.6[d]	
		142.6[e]	
	$[C_2C_1im][PF_6]$	191.8[a]	160.0 [141]
		144.8[b]	
		138.7[c]	
		144.6[d]	
		128.5[e]	
Zhong and co-workers	$[C_2C_1im][NTf_2]$	142.2	134-141 [96, 103, 139]
	$[C_4C_1im][NTf_2]$	138.1	134-155 [96, 103, 139]
	$[C_6C_1im][NTf_2]$	148.5	139 [139], 173 [103]
	$[C_8C_1im][NTf_2]$	156.8	149 [139], 192 [103]

[a]gpFC; [b]gpSC; [c]AIMD-c; [d]AIMD-1; [e]AIMD-b charges defined in footnotes of Table 1.

Borodin [106], and more recently Zhong and co-workers [72], estimated enthalpies of vaporization for the same family of ILs and presented a comparison of their results with previous published data.

As it can be seen from the values collected in Table 4, a large discrepancy of values exists for the same IL, *e.g.* $[C_2C_1im][NTf_2]$ or $[C_4C_1im][NTf_2]$, which is a result of different computational strategies, *i.e.*, by the different parameters from force fields and different values of the total charges in the cation and in the anion for the same ILs. The latter argument is supported by the large difference in the enthalpies of vaporization of $[C_4C_1im][PF_6]$ and $[C_4C_1im][PF_6]$ calculated with total charges close to unity or close to ± 0.8*e* reported by Zhang and Maginn [77]. Nevertheless, values obtained by Koddermann, Batista, Borodin and Zhong and their co-workers are similar, but only for a few cases the calculated results are in close agreement with the experimental data reported until now. Unfortunately, in addition to problems related with the choice of the best simulation strategy, difficulties in the experimental measurement of enthalpies of vaporization lead to the possible existence of inaccurate experimental data, and results obtained by simulation cannot be fully validated (differences can be up to 50 kJ/mol).

In literature, it is also possible to find values for the enthalpy of vaporization for pyridinium-based ILs calculated by Bandrés and co-workers [74], with maximum deviation of ~ 11% from experimental results, and for guanidinium-based ILs calculated by Klähn and co-workers [107], with maximum deviation of ~13% from the experimental ones.

From the analysis of the enthalpies of vaporization available for some families of ILs, it is clear both from the computational and from the experimental studies that an increase of the alkyl chain length of the cations leads to an increase of ΔH^{vap} (Table 4).

Viscosity

Viscosity, η, is a key transport property for industrial purposes, required for the design of process units. Its influence is evident on, for example, the behavior of ILs as lubricants and on mass and heat transfer processes. ILs present values of viscosity significantly higher than those for water or for organic solvents, *e.g.* at T=298.15 K, η(water) = 0.89 cP and η(methanol) = 0.54 cP, while $\eta([C_4C_1im][SCN])$ = 64.81 cP and $\eta([C_4C_1im][C(CN)_2])$ = 31.80 cP . Large viscosities may be considered as disadvantageous for the use of ILs, in processes involving pumping and mixing, and processes that involve heat and mass transfer [3, 64], while they may be considered quite appealing for other applications, such as, lubrication. Changes in temperature, pressure and also in the cation or in the anion that compose the IL will influence directly its viscosity. Impurities such as water were found to have an important influence on the viscosity of ILs and hence on their performance [64]. Though there is still limited available experimental data in literature, MD simulations have been performed. Hess [108], and more recently Tenney and Maginn [109], have discussed new strategies based on classical MD simulations for the calculation of viscosity. Essentially, viscosities can be estimated by EMD simulations, using a Green-Kubo integral (Equation 4) or Einstein relation (Equation 5) to relate fluctuations of off-diagonal elements of pressure tensor to viscosity, at specific limit conditions, such as in Equation 6. This obliges many simulation steps, *i.e.*, very long simulation runs and concomitant storage of large trajectory files, to achieve good statistics.

$$\eta = \frac{V}{k_B T}\int_0^{\infty} \langle P_{\alpha\beta}(0) P_{\alpha\beta}(t)\rangle dt \quad (4)$$

$$\eta = \lim_{t\to\infty} \frac{V}{2tk_B T}\left\langle \left[\int_0^t P_{\alpha\beta}(t')dt'\right]^2 \right\rangle \quad (5)$$

$$\eta = \frac{V}{10k_B T}\int_0^{\infty}\langle P_{ij}^{os}(0)P_{ij}^{os}(t)\rangle dt \qquad (6)$$

$$P_{ij}^{os} = \frac{P_{ij}+P_{ji}}{2} - \delta_{ij}\left(\frac{1}{3}\sum_k P_{kk}\right)$$

In equations 4-6, V is the volume of the system, k_B is the Boltzmann constant, T is the temperature, t is the time and P is the pressure tensor. In the case of NEMD simulations, the response of the system to an external perturbation (shear strain) is used to calculate viscosity through Navier-Stokes equations. The most widely used nonequilibrium approach for viscosity calculations at a given shear rate, $\eta(\dot{\gamma})$, is the SLLOD algorithm [110], which imposes a shear strain on the system and measures the resulting steady state stress (Equation 7) [108, 109].

$$\eta\left(\dot{\gamma}\right) = -\frac{P_{ij}}{\dot{\gamma}} \qquad (7)$$

Nonetheless, Maginn and co-workers [19, 111] discussed the use and application of reverse nonequilibrium MD (RNEMD) to estimate the viscosity of ILs. The RNEMD method imposes the hard-to-measure heat flux and computes the resulting easy-to-measure shear rate or velocity profile, promoting the convergence of the viscosity calculation (Equation 8), where j is the imposed momentum flux, p_{total} is the total exchanged momentum and L defines the length of the simulation box along an axis.

$$j_{xz}\left(p_x\right) = \frac{p_{total}}{2tL_xL_y}, \qquad \eta\left(\dot{\gamma}\right) = -\frac{j_{xz}}{\dot{\gamma}} \qquad (8)$$

The authors were able to conclude that though RNEMD successfully predicts viscosities for several ILs, (agreeing well with the SLLOD and EMD results, at low shear), only under very specific conditions should it be preferably considered, presenting underestimated viscosities at high shear when compared with those calculated with the SLLOD algorithm.

Yan [83], Borodin [106], Van Oanh [112], Zhong [72] and Liu [73] and their co-workers, are among those who used EMD to estimate the viscosity of imidazolium-based ILs. Ghatee and co-workers [74], determined viscosities for some iodide-based ILs (with maximum deviation of 37%). Other authors, *e.g.*, Zhao [113] or Van Oanh [112] and their co-workers, used NEMD approaches for calculating viscosities of 1-butyl-3-methylimidazolium hexafluorophosphate ($[C_4C_1im][PF_6]$), 1-methyl-3-ethylimidazolium bis(trifluoromethane)sulfonamide ($[C_2C_1im][N(SO_2CF_3)_2]$) and 1-ethyl-3-methylimidazolium bis(trifluoromethanesulfonyl)

Table 5. Calculated and experimental viscosities, at different temperatures.

Approach	Author(s)	Ionic Liquid	T / K	η_{this} /(mPa.s)	η_{exp} /(mPa.s)
EMD	Borodin	$[C_4C_1im][CF_3SO_3]$	298	90[a]	84.2 [142]
		$[N_{4111}][NTf_2]$		93[a]	99 [143]
		$[pyr_{14}][NTf_2]$		78[a]	75.7 [143]
		$[C_2C_1im][NTf_2]$		31.2[a]	32.2 [144]
	Ghatee and co-workers	$[C_4C_1im][I]$	298	26.7[b]	28.98
		$[C_6C_1im][I]$		28.2[b]	40.25
		$[C_8C_1im][I]$		35.3[b]	55.68
	Liu and co-workers	$[C_4C_1im][NTf_2]$	298	28[b]	5.1
	Van-Oanh and co-workers	$[C_2C_1im][NTf_2]$	500	3.47[b]	
	Yan and co-workers	$[C_2C_1im][NO_3]$	400	4.74[a] 6.84[b]	4.42
	Zhao and co-workers	$[C_4C_1im][PF_6]$	300	127[b]	
	Zhong and co-workers	$[C_2C_1im][NTf_2]$	353	8.3[b]	7.7 [143]
		$[C_4C_1im][NTf_2]$		12.6[b]	9.2 [104]
		$[C_6C_1im][NTf_2]$		15.5[b]	10.8 [143]
		$[C_8C_1im][NTf_2]$		18.5[b]	12.7 [143]
NEMD	Van-Oanh and co-workers	$[C_2C_1im][NTf_2]$	500	3.6[b]	
RNEMD	Zhao and co-workers	$[C_4C_1im][PF_6]$	298	139.6[b]	228.8 [142]

[a]Polarizable force field
[b]Non-polarizable force field

imide ([C_2C_1im][NTf_2]). Some of these data are compiled in Table **5**. From the results therein reported, the trend that stands out is that in general, results from EMD and NEMD simulations were found to overestimate the experimental viscosity data, and that as the cation alkyl chain length increases, viscosity values also increase. Liu and co-workers [73] demonstrated also the dependence of viscosity with temperature. As expected, as the temperature increases the values of the viscosity decrease. Finally, adding the systematic overestimation of viscosity values to the great computational efforts required for their calculation clearly suggests that improvements of the methods to compute viscosity of ILs are still required.

It was mentioned before that NEMD should be preferably used for the estimation of transport properties, but from the analysis of the studies described above, it is perceived that acceptable results can be also obtained by using EMD formalism. In fact, as it can be seen in Table **5**, the viscosities calculated by Van-Oanh and co-workers [112] for [C_2C_1im][NTf_2] IL with the EMD formalism or with the NEMD approach differ by only 0.13 cP (0.13 mPa·s) at T≒500K.

Diffusion Coefficients

Diffusion coefficient (D) is a transport property, which is important in applications involving mass transfer. This is another property that can also be used to validate force fields, similar to what is done with density but, in opposition to the latter, available experimental values of diffusion coefficients for ILs are scarce in the literature. The diffusion coefficient may be described by the Stokes-Einstein equation, Eq. 9 considering mean square displacements at very large times, showing a great dependence on the viscosity. Similarly to viscosity, long MD simulations are required to obtain accurate values of D due to the slow dynamics that characterize the ILs.

$$D_i = \frac{1}{6}\lim_{t\to\infty}\frac{d}{dt}\left\langle\left[\vec{r}_i(t)-\vec{r}_i(0)\right]^2\right\rangle \quad (9)$$

Margulis [66], Aparicio [114], Borodin [106], Zhong [72], Liu [73] and their co-workers calculated using MD simulations the diffusion coefficients for different imidazolium-based ILs while Kläbn and co-workers [107] calculated the same property for guanidinium-based ILs. Their results are shown in Table 6 and it is demonstrated that the diffusion coefficients for both the cation and anion decrease with the increase of alkyl chain length. The temperature dependence of diffusion coefficients was predicted by Liu and co-workers [73], for the following ILs: 1-butyl-3-methylimidazolium bis[(perfluoroethyl)sulfonyl] imide ([C_4C_1im][PF_2]), 1-butyl-3-methylimidazolium bis (trifluoromethanesulfonyl)imide ([C_4C_1im][NTf_2]), 1-butyl-2,3-dimethylimidazolium bis(trifluoromethanesulfonyl) imide ([$C_4C_1C_1$im][NTf_2]), 1-butyl-1-methylpyrrolidinium bis(trifluoromethanesulfonyl)imide, and *N*-butyl-*N,N,N*-trimetylammonium bis(trifluoromethanesulfonyl)imide, ([N_{4111}][NTf_2]), and was found to be well described by the Arrhenius temperature dependence, *i.e.*, there is a linear dependence of log D with the inverse of temperature (1/T).

Table 6. Calculated and experimental diffusion constants, at different temperatures.

Author(s)	Ionic Liquid	T / K	D^+_{sim} /(m²/s)	D^-_{sim} /(m²/s)	D^+_{exp}/(m²/s)	D^-_{exp}/(m²/s)
Aparicio and co-workers	[C_2C_1im][TOS]	318	5.82×10^{-11}	2.69×10^{-11}		
Borodin	[C_4C_1im][BF_4]	298	0.101×10^{-10}	0.105×10^{-10}	0.145×10^{-10} [142]	0.134×10^{-10} [142]
	[pyr_{14}][NTf_2]		0.119×10^{-10}	0.104×10^{-10}	0.177×10^{-10}	0.142×10^{-10}
	[C_4C_1im][PF_6]		0.032×10^{-10}	0.028×10^{-10}	0.069×10^{-10} [142]	0.0515×10^{-10} [142]
	[C_2C_1im][NTf_2]		0.516×10^{-10}	0.347×10^{-10}	0.495×10^{-10} [145]	0.309×10^{-10} [145]
	[C_4C_1im][NTf_2]		0.289×10^{-10}	0.196×10^{-10}	0.275×10^{-10} [142]	0.218×10^{-10} [142]
	[C_6C_1im][NTf_2]		0.149×10^{-10}	0.144×10^{-10}	0.168×10^{-10} [144]	0.153×10^{-10} [144]
Margulis and co-workers	[C_4C_1im][PF_6]	298	1.42×10^{-11}	1.28×10^{-11}	6.7×10^{-11} [143]	5.7×10^{-11} [143]
Kläbn and co-workers	AP-N	298	1.3×10^{-12}	2×10^{-12}	2.9×10^{-12}	2.9×10^{-12}
	AP-C		0.5×10^{-12}	0.5×10^{-12}	3.6×10^{-12}	4.3×10^{-12}
	CM-N		0.3×10^{-12}	0.3×10^{-12}	1.3×10^{-12}	1.6×10^{-12}
Zhong and co-workers	[C_4C_1im][PF_6]	353	4.7×10^{-11}	3.2×10^{-11}	6.7×10^{-11} [143]	5.7×10^{-11} [143]
	[C_2C_1im][NTf_2]		18.5×10^{-11}	10.2×10^{-11}	22×10^{-11} [143]	14×10^{-11} [143]
	[C_4C_1im][NTf_2]		10.9×10^{-11}	7.8×10^{-11}	15×10^{-11} [143]	13×10^{-11} [143]
	[C_6C_1im][NTf_2]		6.9×10^{-11}	6.2×10^{-11}	12×10^{-11} [143]	11×10^{-11} [143]
	[C_8C_1im][NTf_2]		4×10^{-11}	4×10^{-11}	9×10^{-11} [143]	8.8×10^{-11} [143]

All mentioned simulations produced values that underestimate the experimental results which were found to be approximately one third of the latter ones. Deviations between experimental and simulation results have been suggested to be caused by some inaccuracies of force fields. Importantly, it is possible to conclude from the results in Table 6 that the simulations conducted by Borodin [106] with a polarizable force field, yield values that are closer to the experimental ones [64, 86] than those calculated with a non-polarizable force-field. This suggests that polarizable force fields are essential for the calculation of diffusion coefficients for ILs. Unfortunately, as mentioned above, clear conclusions are not possible since the calibration of the computational procedures suffers from the lack of reliable experimental data for this property.

Surface Tension

This is an important property that measures the cohesive forces between liquid molecules present at a surface between the coexisting liquid and vapor phases, and also allows one to explore different types of segregation/orientation that occur at an ionic/molecular level, very important in the evaluation of complex molecules, such as ILs [115]. It is, then, a property related with the mass transfer efficiency for gas-liquid / liquid-liquid extraction processes and multiphase homogeneous catalysis, and has scarcely been studied. As for viscosity, impurities can affect surface tension, especially in the case of hydrophobic ILs as shown recently by Freire and co-workers [116]. Although it seems that the hydrophobic or hydrophilic nature of ILs has some relevance on surface tension, the influence of water (as impurity) is not very clear [64].

Bhargava and Balasubramanian [49] estimated the surface tension for $[C_4C_1im][PF_6]$ through MD simulations by using the formula of diagonal components of the pressure tensor P_{ii}, as demonstrated in Equation 10 where L_z is the length of the simulation box in the z direction.

$$\gamma = -\frac{L_z}{4}\left(P_{xx} + P_{yy} - 2P_{zz}\right) \qquad (10)$$

In their work, Bhargava and co-workers considered a refined force field with charges on the cation and on the anion of ±0.8*e* based on the AMBER/OPLS type potential parameters for the intramolecular interactions by Canongia-Lopes and co-workers [24], c.f. Table 1. The authors obtained a value for the surface tension of 47 mN/m which is in good agreement with the experimental result of 42.3 mN/m. Canongia Lopes and co-workers [24], considered charges on the cation and on the anion of ±1.0*e*, and using the same equation they obtained a much higher value (γ=74 mN/m) than that calculated by Bhargava and Balasubramanian.

Following the same methodology, Heggen and co-workers [117] studied the impact on the calculated surface tension values for $[C_4C_1im][PF_6]$ of running the MD simulations with different simulation packages (YASP [118] or GROMACS [119]), and considering different treatments for the electrostatics (particle-mesh Ewald, PME, or reaction field, RF). They found that the calculation of surface tension values with bond constraints lead to different results when YASP/RF or GROMACS/RF were considered. For instance, at T=300K, the surface tensions calculated by these codes are 37.3 and 49.0 mN/m, respectively, while the experimental result is 43.5 mN/m. The results obtained with YASP/RF underestimated systematically the experimental values by about 20% in all range of temperatures studied, decreasing as the temperature increase. However, with GROMACS/RF, the calculated results overestimate the experimental ones in the order of 13%. Releasing bond constraints, the YASP code with RF treatment of the electrostatics was able to give a value closer to the experimental result (44.7 mN/m, *i.e.*, a slight overestimation) while Gromacs/RF, with constraints, and Gromacs/RF, without constraints, give practically the same result (49.0 vs 49.3 mN/m, respectively). A much better value was calculated with GROMACS, γ=46.4 mN/m, but using PME. The latter result is almost identical to that calculated by Bhargava and Balasubramanian (see above).

González-Melchor and co-workers [120] computed the surface tension for some ILs by running MD simulations with the aim of studying the size effects of the ions in the surface tension. Interestingly, it was found that the surface tensions of the ILs, considered in that work, decreased with the increase of cation to anion asymmetry. More recently, Pensado and co-workers [121] performed MD simulations, based again on the AMBER/OPLS-AA force field, for interpreting the effect of the length of the alkyl side chain and the presence of a polar hydroxyl group at the end of the side chain, on the surface properties, including the surface tension, of the following ionic liquids: 1-ethyl-3-methylimidazolium tetrafluoroborate ($[C_2C_1im][BF_4]$), 1-(2-hydroxyethyl)-3-methylimidazolium tetrafluoroborate ($[C_2OHC_1im][BF_4]$), 1-octyl-3-methylimidazolium tetrafluoroborate ($[C_8C_1im][BF_4]$) and 1-(8-hydroxyoctyl)-3-methylimidazolium tetrafluoroborate ($[C_8OHC_1im][BF_4]$). The calculated values for these ILs were, respectively, 39.9 mN/m (against 44 mN/m from experimental work), 55.5 mN/m (against 56.9 mN/m from experimental work), 35.6 mN/m and 27.2 mN/m (against 24.7 mN/m from experimental work). The maximum deviation with respect to the experimental data was only 10%. They concluded also from their results that the increase of the length lowered the values calculated for the surface tension but the introduction of the polar hydroxyl group was found to have an opposite effect (surface tension values increased), which was related with the increase of the electrostatic and repulsion-dispersion contributions.

STRUCTURAL DATA

MD simulations can be used to successfully predict properties other than transport and thermodynamic ones. The structures of ILs can also be studied by theoretical means and a common way to do this, is through the estimation of the radial distribution functions (RDFs or g(x)), which gives information concerning the structural organization of a system. More specifically, this function gives the probability of finding a particle at the distance r from another particle (considered as the reference particle) and it is commonly used to aid the interpretation of the experimental results, and for this reason is found in most studies where simulation and experimental means are used to complement each other in the prediction of structural data.

$$g(r) = \frac{n(r)}{4\pi r^2 \rho dr} \quad (11)$$

Bhargava and Balasubramanian [49], calculated RDFs for anion-anion and cation-anion interactions in the 1-butyl-3-methylimidazolium hexafluorophosphate ($[C_4C_1im][PF_6]$) ionic liquid. The idea was to understand the local structural effects in the IL and also check the quality of their refined potential, which was done by comparison with the intermolecular structure in the liquid obtained from ab initio molecular dynamics (AIMD) simulation. Due to the consideration of different force field parameters in the calculations, the positioning and the magnitude of the RDF peaks differed visibly from those calculated with the original force field introduced by Canongia-Lopes and co-workers [12]. For the same $[C_4C_1im][PF_6]$ IL, Margulis and co-workers [66] also calculated RDFs between the cation and anions. RDFs were computed as well for 1-ethyl-3-methylimidazolium hexafluorophosphate ($[C_2C_1im][PF_6]$) [89], 1-ethyl-3-methylimidazolium tetrafluoroborate ($[C_2C_1im][BF_4]$) [67], and 1,3-dimethylimidazolium bis (trifluoromethanesulfonyl)imide ($[C_1C_1im][NTf_2]$) [122]. In these studies, it was possible to identify contacts (hydrogen bonds) between the hydrogen atoms from the imidazolium cation and the fluorine atoms from the anions that compose the ILs. Though these hydrogen bonds are established by different hydrogen atoms from the imidazolium cation with the anion's atoms, the acidic hydrogen in the ring revealed a stronger, but yet weak, interaction with the halogen atoms from both anions. Simultaneously, strong Coulomb interaction was found between the acidic carbon of the imidazolium cation and the boron and phosphorous atoms from the anions. In the study of Alavi and co-workers [90], the same kind of interactions was observed for the anion Br^-, from 1-n-butyl-4-amino-1,2,4-triazolium bromide ionic liquid.

It is worthwhile to mention the work developed by Canongia Lopes and co-workers [14], who, through the estimation of RDFs, demonstrated the complex microscopic structure of ILs that is characterized by the existence of different domains/regions, with different polarities, which has been considered as reference for many studies since then.

The crystal structure of ILs, namely, dimensions (a, b, c) and director angles (α, β, γ) of the unit cell, have also been tentatively predicted by means of MD simulations. Canongia Lopes and co-workers [24] attempted to predict the crystal structure of several ILs, $[C_1C_1im][Cl]$, $[C_2C_1im][Cl]$, $[C_2C_1im][NO_3]$ and $[C_2C_1im][PF_6]$, based on the dimensions and occupancy of the unit cells of each crystalline structure taken from the Cambridge Structural Database (CSD), and considering classical simulations in the NPT ensemble and their force field based on AMBER/OPLS-AA parameters. The results obtained agreed well with the experimental ones, and the highest deviation, around 3.5 %, was observed for the value of the β vector. In following works [123, 124], the prediction of the crystal structure was attempted for *n*-butylpyridinium chloride ($[C_4py][Cl]$), tetradecylphosphonium bromide ($[P_{10,10,10,10}][Br]$), tetramethylammonium dicyanamide ($[N_{1,1,1,1}][C(CN)_2]$), triphenylphosphonium bis(fluorosulfonyl) amide ($[PH(C_6H_5)_3][N(SO_2F)_2]$), sodium *trans*-bis(perfluoro-n-butylsulfonyl)amide ($[Na][N(SO_2C_2F_5)_2]$), potassium *trans*-bis(perfluoro-*n*-butylsulfonyl)amide and potassium *cis*-bis(perfluoro-*n*-butylsulfonyl)amide ($[K][N(SO_2C_2F_5)_2]$) and, finally, for 1,3-dimethoxy-2-ethylimidazolium tris(pentafluoroethyl)trifluorophosphate ($[(OMe)_2C_1im][PF_3(C_2F_5)_3]$). Using the methodology applied in previous work [12], it was possible to obtain results in good agreement with the experimental ones (obtained through X-ray experiments), for cell vector lengths and cell vector angles, with deviations ranging between 2% and 4%. The prediction of the crystal structure was considered as a good test to develop and to validate the force fields used for the different ILs. Jayaraman and Maginn [94], predicted the crystal structure of $[C_4C_1im][Cl]$ with two different potentials, namely, that developed by Canongia Lopes and co-workers [24], based on OPLS parameters, and that developed by Cadena and Maginn [69], based on CHARMM force field. The results calculated with any of the two force fields were found to reproduce well the experimental ones with a deviation of less than 1%. Nevertheless, when the two possible polymorphs of this IL were studied, only the second one was able to reproduce both structures in a stable form. Please notice that in this IL the anion is just an isolated atom and the potential of Maginn and co-workers considers charges of $\pm 1.0e$ as in the potential of Canongia-Lopes and co-workers. A recent work from Zhang and Maginn [77] reported not only densities, enthalpies of vaporization and melting points of $[C_2C_1im][PF_6]$ and $[C_4C_1im][PF_6]$ but also the prediction of their crystal structure. The simulations were performed at T=173 K through NVT and NPT ensembles, considering GAFF force field and five different sets of atomic charges. They found that the lattice parameters are not affected by the differences in ILs' atomic charges. The calculated results are in good agreement with the experimental ones, with a maximum deviation of 4% in the case of $[C_3C_1im][PF_6]$ and a maximum deviation of 2.5% in the case of $[C_2C_1im][PF_6]$).

Borodin [106] in his extensive study concerning the prediction of thermodynamic, transport and structural properties of ILs, was also able to obtain very good results for the crystal structure of the ILs studied with deviations not more than 2.5% from the results obtained through X-ray measurements. This author used a many-body polarizable force field and considered the NPT ensemble to model the $[C_2C_1im][NTf_2]$, $[pyr_{13}][NTf_2]$, $[pyr_{14}][NTf_2]$ and $[C_2C_1im][CF_3SO_3]$ ILs, with initial dimensions and occupancy of the unit cells of each crystalline structure taken from the CSD.

DISCUSSION

The first polarizable force field for modeling ILs was published by Yan and co-workers [83]. In that work, polarizable and non-polarizable force fields were compared, and results showed differences in the way how the system dynamics were reproduced. Their work was followed by others [52, 106, 125, 126], and reviews [3, 58] about the use of polarizable force fields in classical simulations have been published. A general conclusion concerning the use of polarizable force fields is that, comparing with the non-polarizable ones, the structural arrangements of the ILs studied were not greatly affected, but systems were accelerated, which promoted a better description of the slow dynamic of ILs. A concomitant result was the observation of

a decrease in the values calculated for the viscosity and an increase in the values calculated for the diffusion coefficient.

Most of the works reported in the present review considered non-polarizable force fields since they run much faster than simulations employing polarizable FFs. Nevertheless, the diffusion constants were underestimated, the viscosities were overestimated and quite good agreements between calculated and experimental results were found for the densities and the surface tensions of ILs. The usage of polarizable force fields in some cases lead to calculated results that are closer to the experimental ones (e.g. Tables **5** and **6**) which is probably related with the fact that the charges on the ILs' cations and on the ILs' anions vary with the nature of the charged units and with the number and the nature of the surrounding units, and with the fact that the total charges in the ILs constituting ions seem to be often different from unity, which was considered only in some of the non-polarizable simulations reviewed here. Thus, the point charges seem to have a very important role in the quality of the thermodynamic properties calculated with MD simulation. Most of non-polarizable force fields used in the studies reviewed here considered several different strategies for calculating the atomic charges used for each IL constituting cation or anion. The methods based on the fitting of the electrostatic potential in the vicinity of a molecule (ESP), or restrained electrostatic potential (RESP), and the method ESP but using a grid base (CHelpG) are the ones most used (being the latter the most considered in the studies reported in this work). Nevertheless, is has been also applied the Blöchl method [52, 79, 127], which derives the partial charges under bulk conditions, by fitting the system expressed in multipole moments. The latter method takes into account periodic boundary conditions, which is very convenient for the calculation of the charge distribution of an IL in the liquid phase and for the assignment of its partial charges [58, 127]. Chaban and co-workers [125], on other hand, determined a charge scaling factor that matches experimental properties of ILs. It was also shown that its application in non-polarizable force field will improve its quality and the prediction of ILs' properties. In a recent work, Zhang and Maginn [77], derived atomic charges using several different strategies and compared the calculated results for several properties with experimental data, being able to conclude that the consideration of charges resulting from a fitting of the charges in a crystal phase yielded quite good static and dynamic properties, and therefore consisting in a simple and reliable methodology.

In summary, the use of polarizable force fields would be preferred in all classical simulations but their consideration seems to be crucial only if one wants to calculate very accurate dynamic properties. The price to pay for the usage of the polarizable force fields is the much higher computational effort needed to perform the simulations, which is a very important issue to take into account. In fact, for most of the properties analyzed in this review, the consideration of a non-polarizable FF together with total charges in the ions of $\sim\pm$ 0.8*e* seems to be a very good choice in terms of the ratio between the quality of results and the computational resources required for their determination.

Table 7. accuracy of MD simulations for calculating structural and thermodynamic properties of ILs with respect to available experimental results.

Calculated Property	Comparison to Experimental Results
Density	Very Good
Melting Point	Good
Enthalpy of Vaporization	?[a]
Viscosity	Overestimated
Diffusion Coefficients	Underestimated
Surface Tension	Overestimated/Underestimated
Structural Data	Very Good Complement to Information Retrieved from Experimental Work

[a]Hard to be defined due to several different experimental results determined by different authors for the same IL.

CONCLUSIONS

In this work it was highlighted the importance of characterizing ionic liquids due to their potential in a vast range of applications. MD simulations, among other computer approaches, proved to be very useful for the understanding of the relation between physical and chemical properties with their intrinsic structures. Properties of ILs, such as density, viscosity, diffusivity, melting point, enthalpy of vaporization and surface tension were introduced and their relevance for understanding the behaviors of ILs was analyzed. Studies where these properties were calculated, were used to illustrate the capacities of computational tools to characterize ILs.

It was shown that MD simulations are able to reproduce the properties of systems of ILs with some accuracy (Table **7**). However, due to the time limitations and to the slow dynamic of ILs, calculated values for some properties were found to be systematically over/underestimated (*e.g.* viscosity or diffusion constant) which, in principle, can be overcome by using a polarizable force field. However, due to the lack of reliable experimental data for the enthalpies of vaporization of ILs, it is not easy to understand the adequacy of the present computational strategies for the calculation of this property.

Despite all the efforts made in the field of MD simulations, it is possible to realize (especially in the case of viscosity) that a lot of improvements need to be made. Along with technology improvements, it is important to highlight that a straight line between experimental and theoretical procedures must exist. Experimentally, caution is needed in the purification of ILs in order to minimize impurities (water and others) that affect the determination of their properties. This constitutes a problem for the simulations since, without available accurate experimental data, it is quite difficult to calibrate computational strategies (*e.g.* force fields) for calculation of properties of ILs. We do hope that the present review will trigger new experimental and computational studies devoted to the determination of thermodynamic properties of new ILs.

CONFLICT OF INTEREST

The author(s) confirm that this article content has no conflict of interest.

ACKNOWLEDGEMENTS

The authors are thankful for financial support from Fundação para a Ciência e a Tecnologia for Projects PTDC/EQU-FTT/102166/2008 and Pest-C/CTM/LA0011/2011 (CICECO), for Programa Ciência 2007, and for PhD grant (SFRH/BD/74551/2010) of Marta Batista.

REFERENCES

[1] Walden, P. Bulletin de l'Académie Impériale des Sciences de St.-Pétersbourg, **1914**, *8*, 405-422.

[2] Kokorin, A. Ionic liquids: Theory, properties, new approaches. InTech, Croatia, **2011**.

[3] Kirchner, B. Topics in current chemistry: Ionic liquids, Springer, Germany, 290, **2010**.

[4] Gardas, R.L.; Coutinho, J.A.P. Group contribution methods for the prediction of thermophysical and transport properties of ionic liquids. *AIChE J.*, **2009**, *55*, 1274-1290.

[5] Bini, R.; Malvaldi, M.; Pitner, W.R.; Chiappe, C. QSPR correlation for conductivities and viscosities of low-temperature melting ionic liquids. *J. Phys. Org. Chem.*, **2008**, *21*, 622-629.

[6] Carvalho, P.J.; Coutinho, J.A.P. On the nonideality of CO_2 solutions in ionic liquids and other low volatile solvents. *J. Phys. Chem. Lett.*, **2010**, 1, 774-780.

[7] Freire, M.G.; Neves, C.; Ventura, S.P.M.; Pratas, M.J.; Marrucho, I.M.; Oliveira, J.; Coutinho, J.A.P.; Fernandes, A.M. Solubility of non-aromatic ionic liquids in water and correlation using a QSPR approach. *Fluid Phase Equilib.*, **2010**, *294*, 234-240.

[8] Coutinho, J.A.P.; Carvalho, P.J.; Oliveira, N.M.C. Predictive methods for the estimation of thermophysical properties of ionic liquids. *RSC Adv.*, **2012**, *2*, 7322-7346.

[9] Torrecilla, J.S.; Palomar, J.; Lemus, J.; Rodriguez, F. A quantum-chemical-based guide to analyze/quantify the cytotoxicity of ionic liquids. *Green Chem.*, **2010**, *12*, 123-134.

[10] Freire, M.G.; Carvalho, P.J.; Santos, L.M.N.B.F.; Gomes, L.R.; Marrucho, I.M.; Coutinho, J.A.P. Solubility of water in fluorocarbons: Experimental and COSMO-RS prediction results. *J. Chem. Thermodyn.*, **2010**, *42*, 213-219.

[11] Lopes, C.J.N.; Pádua, A.A.H. Molecular force field for ionic liquids composed of triflate or bistriflylimide anions. *J. Phys. Chem. B*, **2004**, *108*, 16893-16898.

[12] Lopes, J.N.C.; Deschamps, J.; Padua, A.A.H. Modeling ionic liquids using a systematic all-atom force field. *J. Phys. Chem. B*, **2004**, *108*, 2038-2047.

[13] Maginn, E.J. Molecular simulation of ionic liquids: Current status and future opportunities. *J. Phys. Condensed Matt.*, **2009**, *21*, 373101-373118.

[14] Lopes, C.J.N.; Gomes, C.M.F.; Pádua, A.A.H. Nonpolar, polar, and associating solutes in ionic liquids. *J. Phys. Chem. B*, **2006**, *110*, 16816-16818.

[15] Lopes, J.N.A.; Padua, A.A.H. Nanostructural organization in ionic liquids. *J. Phys. Chem. B*, **2006**, *110*, 3330-3335.

[16] Shimizu, K.; Costa Gomes, M.F.; Pádua, A.A.H.; Rebelo, L.P.N.; and Canongia Lopes, J.N. Three commentaries on the nano-segregated structure of ionic liquids. *J. Mol. Struc.: Theochem*, **2010**, *946*, 70-76.

[17] Batista, M.L.S.; Neves, C.M.S.S.; Carvalho, P.J.; Gani, R.; Coutinho, J.A.P. Chameleonic behavior of ionic liquids and its impact on the estimation of solubility parameters. *J. Phys. Chem. B*, **2011**, *115*, 12879-12888.

[18] Hunt, P.A. The simulation of imidazolium-based ionic liquids. *Mol. Simulat.*, **2006**, *32*, 1-10.

[19] Maginn, E.J. Atomistic simulation of the thermodynamic and transport properties of ionic liquids. *ACC. Chem. Res.*, **2007**, *40*, 1200-1207.

[20] Bhargava, B.L.; Balasubramanian, S.; Klein, M.L. Modelling room temperature ionic liquids. *Chem. Commun.*, **2008**, *29*, 3339-3351.

[21] Izgorodina, E.I. Towards large-scale, fully ab initio calculations of ionic liquids. *Phys. Chem. Chem. Phys.*, **2011**, *13*, 4189-4207.

[22] Bhargava, B.L.; Yasaka, Y.; Klein, M.L. Computational studies of room temperature ionic liquid-water mixtures. *Chem. Commun.*, **2011**, *47*, 6228-6241.

[23] Bessac, F.; Maseras, F. DFT Modeling of reactivity in an ionic liquid: How many ion pairs?, *J. Comput. Chem.*, **2008**, *29*, 892-899.

[24] Lopes, C.J.N.; Deschamps, J.; Pádua, A.A.H. Modeling ionic liquids using a systematic all-atom force field. *J. Phys. Chem. B*, **2004**, *108*, 2038-2047.

[25] Wang, Y.; Feng, S.; Voth, G.A. Transferable coarse-grained models for ionic liquids. *J. Chem. Theory. Comput.*, **2009**, *5*, 1091-1098.

[26] Wittich, B.; Deiters, U.K. Calculating thermodynamic properties of an ionic liquid with monte carlo simulations with an orthorhombic and a cubic simulation box. *J. Phys. Chem. B*, **2010**, *114*, 8954-8960.

[27] Cramer, C.J. Essentials of computational chemistry - Theories and models. 2nd John Wiley and Sons Ltd, Chichester, West Sussex, England, **2004**.

[28] Marx, D.; Hutter, J. Ab initio molecular dynamics: Basic theory and advanced method, Cambridge University Press **2009**.

[29] Parr, R.G.; Yang, W. Density-functional theory of atoms and molecules, Oxford University Press, New York, **1989**.

[30] Møller, C.; Plesset, M.S. Note on an approximation treatment for many-electron systems. *Phys. Rev.*, **1934**, *46*, 618-622.

[31] Krishnan, R.; Pople, J.A. Approximate fourth-order perturbation theory of the electron correlation energy. *Int. J. Quant. Chem.* **1978**, *14*, 91-100.

[32] Purvis III, G.D. ; Bartlett, R.J. A full coupled-cluster singles and doubles model: The inclusion of disconnected triples. *J. Chem. Phys.*, **1982**, *76*, 1910-1918.

[33] Maurice, D.; Head-Gordon, M. Analytical second derivatives for excited electronic states using the single excitation configuration interaction method: theory and application to benzo[a]pyrene and chalcone. *Mol. Phys.*, **1999**, *96*, 1533-1541.

[34] Gubbins, K.E.; Moore, J.D. Molecular modeling of matter: impact and prospects in engineering. *Ind. Eng. Chem. Res.*, **2010**, *49*, 3026-3046.

[35] Jensen, F. Introduction to computational chemistry, John Wiley & Sons, Ltd.; Chichester, West Sussex, England **2007**.

[36] Metropolis, N.; Rosenbluth, A.W.; Rosenbluth, M.N.; Teller, A.H.; Teller, E. Equation of state calculations by fast computing machines. *J. Chem. Phys.*, **1953**, *21*, 1087-1092.

[37] Kroese, D.P.; Taimre, T.; Botev, Z.I. Handbook of Monte Carlo Methods, John Wiley & Sons, Inc, Hoboken, New Jersey, **2011**.

[38] Haile, J.M. Molecular dynamics simulation: Elementary methods, John Wiley & Sons, Inc, **1992**.

[39] Shah, J.K.; Brennecke, J.F.; Maginn, E.J. Thermodynamic properties of the ionic liquid 1-n-butyl-3-methylimidazolium hexafluorophosphate from Monte Carlo simulations. *Green Chem.*, **2002**, *4*, 112-118.

[40] Bresme, F.; Alejandre, J. Cavities in ionic liquids. *J. Chem. Phys.*, **2003**, *118*, 4134-4139.

[41] Shi, W.; Maginn, E.J. Atomistic simulation of the absorption of carbon dioxide and water in the ionic liquid 1-n-hexyl-3-methylimidazolium bis(trifluoromethylsulfonyl)imide [hmim]{Tf2N}. *J. Phys. Chem. B*, **2008**, *112*, 2045-2055.

[42] Liu, J.-X.; Bowman, T.L.; Elliott, J.R. Discontinuous molecular dynamics simulation of hydrogen-bonding systems. *Ind. Eng. Chem. Res.*, **1994**, 33, 957-964.

[43] Andersen, H.C. Molecular-dynamics simulations at constant pressure and-or temperature. *J. Chem. Phys.*, **1980**, *72*, 2384-2393.

[44] Nose, S. A unified formulation of the constant temperature molecular-dynamics methods. *J. Chem. Phys.*, **1984**, *81*, 511-519.

[45] Hoover, W.G. Canonical dynamics - equilibrium phase-space distributions. *Phys. Rev. A*, **1985**, *31*, 1695-1697.

[46] Berendsen, H.J.C.; Postma, J.P.M.; Vangunsteren, W.F.; Dinola, A.; Haak, J.R. Molecular-dynamics with coupling to an external bath. *J. Chem. Phys.*, **1984**, *81*, 3684-3690.

[47] Parrinello, M. Rahman, A. Polymorphic transitions in single-crystals - A new molecular-dynamics method. *J. Appl. Phys.*, **1981**, *52*, 7182-7190.

[48] Parrinello, M.; Rahman, A.; Vashishta, P. Structural transitions in superionic conductors. *Phys. Rev. Lett.*, **1983**, *50*, 1073-1076.

[49] Bhargava, B.L. Balasubramanian, S. Refined potential model for atomistic simulations of ionic liquid butim PF6. *J. Chem. Phys.*, **2007**, *127*, 114510-114516.

[50] Buhl, M.; Chaumont, A.; Schurhammer, R.; Wipff, G. Ab initio molecular dynamics of liquid 1,3-dimethylimidazolium chloride. *J. Phys. Chem. B*, **2005**, *109*, 18591-18599.

[51] Kossmann, S.; Thar, J.; Kirchner, B.; Hunt, P.A.; Welton, T. Cooperativity in ionic liquids. *J. Chem. Phys.*, **2006**, *124*, 174506-174518.

[52] Schmidt, J.; Krekeler, C.; Dommert, F.; Zhao, Y.; Berger, R.; Delle Site, L.; Holm, C. Ionic charge reduction and atomic partial charges from first-principles calculations of 1,3-dimethylimidazolium chloride. *J. Phys. Chem. B*, **2010**, *114*, 6150-6155.

[53] Schroeder, C. and Steinhauser, O. The influence of electrostatic forces on the structure and dynamics of molecular ionic liquids. *J. Chem. Phys.*, **2008**, *128*, 224503-224510.

[54] Brooks, B.R.; Bruccoleri, R.E.; Olafson, B.D.; States, D.J.; Swaminathan, S.; Karplus, M. CHARMM - A program for macromolecular energy, minimization, and dynamics calculations. *J. Comput. Chem.*, **1983**, *4*, 187-217.

[55] Jorgensen, W.L.; Tiradorives, J. The OPLS potencial functions for proteins - energy minimizations dor crystals of cyclic-peptides and crambin. *J. Am. Chem. Soc.*, **1988**, *110*, 1657-1666.

[56] Jorgensen, W.L.; Maxwell, D.S.; TiradoRives, J. Development and testing of the OPLS all-atom force field on conformational energetics and properties of organic liquids. *J. Am. Chem. Soc.*, **1996**, *118*, 11225-11236.

[57] Cornell, W.D.; Cieplak, P.; Bayly, C.I.; Gould, I.R.; Merz, K.M.; Ferguson, D.M.; Spellmeyer, D.C.; Fox, T.; Caldwell, J.W.; Kollman, P.A. A 2nd generayion force-field for the simulation of proteins, nuclei-acids and organic-molecules. *J. Am. Chem. Soc.*, **1995**, *117*, 5179-5197.

[58] Dommert, F.; Wendler, K.; Berger, R.; Delle Site, L.; Holm, C.. Force fields for studying the structure and dynamics of ionic liquids: A critical review of recent developments. *Chemphyschem.*, **2012**, *13*, 1625-1637.

[59] McCarty, J.; Lyubimov, I.Y.; Guenza, M.G. Multiscale modeling of coarse-grained macromolecular liquids. *J. Phys. Chem. B*, **2009**, *113*, 11876-11886.

[60] Pérez-Sánchez, G.; Gomes, J.R.B.; Jorge, M. Modelling self-assembly of silica/surfactant mesostructures in the templated synthesis of nanoporous solids. Langmuir, **2013**, *29*, 2387-2396.

[61] Velinova, M.; Sengupta, D.; Tadjer, A.V.; Marrink, S.-J. Sphere-to-rod transitions of nonionic surfactant micelles in aqueous solution modeled by molecular dynamics simulations. Langmuir, **2011**, *27*, 14071-14077.

[62] Chen, Y.; Zimmerman, J.; Krivtsov, A.; McDowell, D.L. Assessment of atomistic coarse-graining methods. *Int. J. Eng. Sci.*, **2011**, *49*, 1337-1349.

[63] Ionic Liquids Database - (IL Thermo). NIST Standard Reference Database #47. 2006, National Institute os Standards and Technology: Gaithersburg, MD, USA.

[64] Aparicio, S.; Atilhan, M.; Karadas, F. Thermophysical properties of pure ionic liquids: Review of present situation. *Ind. Eng. Chem. Res.*, **2010**, *49*, 9580-9595.

[65] Paduszyński, K. and Domańska, U. A new group contribution method for prediction of density of pure ionic liquids over a wide range of temperature and pressure. *Ind. Eng. Chem. Res.*, **2011**, *51*, 591-604.

[66] Margulis, C.J.; Stern, H.A.; Berne, B.J. Computer simulation of a "green chemistry" room-temperature ionic solvent. *J. Phys. Chem. B*, **2002**, *106*, 12017-12021.

[67] Prado, C.E.R.; Freitas, L.C.G. Molecular dynamics simulation of the room-temperature ionic liquid 1-butyl-3-methylimidazolium tetrafluoroborate. *J. Mol. Struc.Theochem*, **2007**, *847*, 93-100.

[68] Batista, M.L.S.; Tomé, L.I.N.; Neves, C.M.S.S.; Rocha, E.M.; Gomes, J.R.B.; Coutinho, J.A.P. The Origin of the LCST on the liquid–liquid equilibrium of thiophene with ionic liquids. *J. Phys. Chem. B*, **2012**, *116*, 5985-5992.

[69] Cadena, C.; Maginn, E.J. Molecular simulation study of some thermophysical and transport properties of triazolium-based ionic liquids. *J. Phys. Chem. B*, **2006**, *110*, 18026-18039.

[70] Morrow, T.I.; Maginn, E.J. Molecular dynamics study of the ionic liquid 1-n-butyl-3-methylimidazolium hexafluorophosphate. *J. Phys. Chem. B*, **2002**, *106*, 12807-12813.

[71] Wang, J.M.; Wolf, R.M.; Caldwell, J.W.; Kollman, P.A.; Case, D.A. Development and testing of a general amber force field. *J. Comput. Chem.*, **2004**, *25*, 1157-1174.

[72] Zhong, X.; Liu, Z.; Cao, D. Improved classical united-atom force field for imidazolium-based ionic liquids: Tetrafluoroborate, hexafluorophosphate, methylsulfate, trifluoromethylsulfonate, acetate, trifluoroacetate, and bis(trifluoromethylsulfonyl)amide. *J. Phys. Chem. B*, **2011**, *115*, 10027-10040.

[73] Liu, H.; Maginn, E.; Visser, A.E.; Bridges, N.J.; Fox, E.B.; Thermal and transport properties of six ionic liquids: an experimental and molecular dynamics study. *Ind. Eng. Chem. Res.*, **2012**, *51*, 7242-7254.

[74] Bandrés, I.; Alcalde, R.; Lafuente, C.; Atilhan, M.; Aparicio, S. On the viscosity of pyridinium based ionic liquids: an experimental and computational study. *J. Phys. Chem. B*, **2011**, *115*, 12499-12513.

[75] Ghatee, M.H.; Zolghadr, A.R.; Moosavi, F.; Ansari, Y. Studies of structural, dynamical, and interfacial properties of 1-alkyl-3-methylimidazolium iodide ionic liquids by molecular dynamics simulation. *J. Chem. Phys.*, **2012**, *136*, 124706-124720.

[76] Shimizu, K.; Tariq, M.; Gomes, M.F.C.; Rebelo, L.P.N.; Lopes, J.N.C. Assessing the dispersive and electrostatic components of the cohesive energy or ionic liquids using molecular dynamics simulations and molar refraction data. *J. Phys. Chem. B*, **2010**, *114*, 5831-5834.

[77] Zhang, Y.; Maginn, E.J. A simple AIMD approach to derive atomic charges for condensed phase simulation of ionic liquids. *J. Phys. Chem. B*, **2012**, *116*, 10036-10048.

[78] Singh, U.C.; Kollman, P.A. An approach to computing electrostatic charges for molecules. *J. Comput. Chem.*, **1984**, *5*, 129-145.

[79] Blochl, P.E. Electrostatic decoupling of periodic images of plane-wave-expanded densities and derived atomic point charges. *J. Chem. Phys.*, **1995**, *103*, 7422-7428.

[80] Besler, B.H.; Merz, K.M.; Kollman, P.A. Atomic charges derived from semiempirical methods. *J. Comput. Chem.*, **1990**, *11*, 431-439.

[81] Breneman, C.M.; Wiberg, K.B. Determining atom-centered monopoles from molecular electrostatic potentials - The need for high sampling density in formamide conformational-analysis. *J. Comput. Chem.*, **1990**, *11*, 361-373.

[82] Bayly, C.I.; Cieplak, P.; Cornell, W.D.; Kollman, P.A. A well-behaved electrostatic potential based method using charge restrainst for deriving atomic charges - The RESP model. *J. Phys. Chem.*, **1993**, *97*, 10269-10280.

[83] Yan, T.Y.; Burnham, C.J.; Del Popolo, M.G.; Voth, G.A.; Molecular dynamics simulation of ionic liquids: The effect of electronic polarizability. *J. Phys. Chem. B*, **2004**, *108*, 11877-11881.

[84] Holbrey, J.D. and Seddon, K.R. The phase behaviour of 1-alkyl-3-methylimidazolium tetrafluoroborates; ionic liquids and ionic liquid crystals. *J. Chem. Soc. Dalton Trans.*, **1999**, *13*, 2133-2139.

[85] Holbrey, J.D.; Reichert, W.M.; Nieuwenhuyzen, M.; Johnston, S.; Seddon, K.R.; Rogers, R.D. Crystal polymorphism in 1-butyl-3-methylimidazolium halides: Supporting ionic liquid formation by inhibition of crystallization. *Chem. Commun.*, **2003**, *14*, 1636-1637.

[86] Weingaertner, H. Understanding ionic liquids at the molecular level: Facts, problems, and controversies. *Angewandte Chemie-Int. Ed.*, **2008**, *47*, 654-670.

[87] Yoo, S.; Zeng, X.C.; Xantheas, S.S. On the phase diagram of water with density functional theory potentials: The melting temperature of ice I[sub h] with the Perdew--Burke--Ernzerhof and Becke--Lee--Yang--Parr functionals. *J. Chem. Phys.*, **2009**, *130*, 221102-221106.

[88] Luo, S.-N.; Strachan, A.; Swift, D.C. Nonequilibrium melting and crystallization of a model Lennard-Jones system. J. Chem. Phys., **2004**, *120*, 11640-11649.

[89] Alavi, S.; Thompson, D.L. Molecular dynamics studies of melting and some liquid-state properties of 1-ethyl-3-methylimidazolium hexafluorophosphate emim PF6. *J. Chem. Phys.*, **2005**, 122, 154704-154716.

[90] Alavi, S.; Thompson, D.L. Simulations of the solid, liquid, and melting of 1-n-butyl-4-amino-1,2,4-triazolium bromide. *J. Phys. Chem. B*, **2005**, *109*, 18127-18134.

[91] Frenkel, D.; Ladd, A.J.C. New Monte-Carlo method to compute the free-energy of arbitrary solids - application to the FCC and HCP phases of hard-spheres. *J. Chem. Phys.*, **1984**, *81*, 3188-3193.

[92] Grochola, G. Constrained fluid lambda-integration: Constructing a reversible thermodynamic path between the solid and liquid state. *J. Chem. Phys.*, **2004**, *120*, 2122-2126.
[93] Hoover, W.G.; Ree, F.H. Use of computer experiments to locate melting transition and calculate entropy in solid phase. *J. Chem. Phys.*, **1967**, 47, 4873-4878.
[94] Jayaraman, S. and Maginn, E.J. Computing the melting point and thermodynamic stability of the orthorhombic and monoclinic crystalline polymorphs of the ionic liquid 1-n-butyl-3-methylimidazolium chloride. *J. Chem. Phys.*, **2007**, *127*, 214504-214518.
[95] Zhang, Y.; Maginn, E.J. A comparison of methods for melting point calculation using molecular dynamics simulations. *J. Chem. Phys.*, **2012**, *136*, 144116-144128.
[96] Esperanca, J.; Lopes, J.N.C.; Tariq, M.; Santos, L.; Magee, J.W.; Rebelo, L.P.N. Volatility of aprotic ionic liquids - A review. *J. Chem. Eng. Data*, **2010**, *55*, 3-12.
[97] Earle, M.J.; Esperanca, J.; Gilea, M.A.; Lopes, J.N.C.; Rebelo, L.P.N.; Magee, J.W.; Seddon, K.R.; Widegren, J.A. The distillation and volatility of ionic liquids. *Nature*, **2006**, *439*, 831-834.
[98] Rebelo, L.P.N.; Lopes, J.N.C.; Esperanca, J.; Filipe, E. On the critical temperature, normal boiling point, and vapor pressure of ionic liquids. *J. Phys. Chem. B*, **2005**, *109*, 6040-6043.
[99] Paulechka, Y.U.; Zaitsau, D.H.; Kabo, G.J.; Strechan, A.A. Vapor pressure and thermal stability of ionic liquid 1-butyl-3-methylimidazolium Bis(trifluoromethylsulfonyl)amide. *Thermochim. Acta*, **2005**, *439*, 158-160.
[100] Rocha, M.A.A.; Bastos, M.; Coutinho, J.A.P.; Santos, L.M.N.B.F. Heat capacities at 298.15K of the extended [CnClim][Ntf2] ionic liquid series. *J. Chem. Thermodyn.*, **2012**, *53*, 140-143.
[101] Liu, Z.P.; Huang, S.P.; Wang, W.C. A refined force field for molecular simulation of imidazolium-based ionic liquids. *J. Phys. Chem. B*, **2004**, *108*, 12978-12989.
[102] Liu, Z.P.; Wu, X.P.; Wang, W.C. A novel united-atom force field for imidazolium-based ionic liquids. *Phys. Chem. Chem. Phys.*, **2006**, *8*, 1096-1104.
[103] Santos, L.M.N.B.F.; Lopes, J.N.C.; Coutinho, J.A.P.; Esperanca, J.M.S.S.; Gomes, L.R.; Marrucho, I.M.; Rebelo, L.P.N. Ionic liquids: First direct determination of their cohesive energy. *J. Am. Chem. Soc.*, **2007**, *129*, 284-285.
[104] Kelkar, M.S.; Maginn, E.J. Calculating the enthalpy of vaporization for ionic liquid clusters. *J. Phys. Chem. B*, **2007**, *111*, 9424-9427.
[105] Koeddermann, T.; Paschek, D.; Ludwig, R. Molecular dynamic simulations of ionic liquids: A reliable description of structure, thermodynamics and dynamics. *ChemPhysChem*, **2007**, *8*, 2464-2470.
[106] Borodin, O. Polarizable force field development and molecular dynamics simulations of ionic liquids. *J. Phys. Chem. B*, **2009**, *113*, 11463-11478.
[107] Klähn, M.; Seduraman, A.; Wu, P. A model for self-diffusion of guanidinium-based ionic liquids: A molecular simulation study. *J. Phys. Chem. B*, **2008**, 112, 13849-13861.
[108] Hess, B. Determining the shear viscosity of model liquids from molecular dynamics simulations. *J. Chem. Phys.*, **2002**, *116*, 209-217.
[109] Tenney, C.M.; Maginn, E.J. Limitations and recommendations for the calculation of shear viscosity using reverse nonequilibrium molecular dynamics. *J. Chem. Phys.*, **2010**, *132*, 014103-014111.
[110] Evans, D.J.; Morriss, G.P. Statistical mechanics of nonequilibrium liquids, Academic, London, **1990**.
[111] Kelkar, M.S.; Maginn, E.J. Effect of temperature and water content on the shear viscosity of the ionic liquid 1-ethyl-3-methylimidazolium bis(trifluoromethanesulfonyl)imide as studied by atomistic simulations. *J. Phys. Chem. B*, **2007**, *111*, 4867-4876.
[112] Van-Oanh, N.-T.; Houriez, C.; Rousseau, B. Viscosity of the 1-ethyl-3-methylimidazolium bis(trifluoromethylsulfonyl)imide ionic liquid from equilibrium and nonequilibrium molecular dynamics. *Phys. Chem. Chem. Phys.*, **2010**, *12*, 930-936.
[113] Zhao, W.; Leroy, F.; Balasubramanian, S.; Mueller-Plathe, F. Shear viscosity of the ionic liquid 1-n-butyl 3-methylimidazolium hexafluorophosphate bmim PF(6) computed by reverse nonequilibrium molecular dynamics. *J. Phys. Chem. B*, **2008**, *112*, 8129-8133.
[114] Aparicio, S.; Alcalde, R.; Garcia, B.; Leal, J.M. High-pressure study of the methylsulfate and tosylate imidazolium ionic liquids. *J. Phys. Chem. B*, **2009**, *113*, 5593-5606.
[115] Tariq, M.; Freire, M.G.; Saramago, B.; Coutinho, J.A.P.; Canongia Lopes, J.N.; Rebelo, L.P.N. Surface tension of ionic liquids and ionic liquid solutions. *Chem. Soc. Rev.*, **2012**, *41*, 829-868.
[116] Freire, M.G.; Carvalho, P.J.; Gardas, R.L.; Marrucho, I.M.; Santos, L.; Coutinho, J.A.P. Mutual solubilities of water and the C(n)mim Tf2N hydrophobic ionic liquids. *J. Phys. Chem. B*, **2008**, *112*, 1604-1610.
[117] Heggen, B.; Zhao, W.; Leroy, F.; Dammers, A.J.; Mueller-Plathe, F. Interfacial properties of an ionic liquid by molecular dynamics. *J. Phys. Chem. B*, **2010**, *114*, 6954-6961.
[118] Tarmyshov, K.B.; Muller-Plathe, F. Parallelizing a molecular dynamics algorithm on a multiprocessor workstation using OpenMP. *J. Chem. Informat. Model.*, **2005**, *45*, 1943-1952.
[119] Lindahl, E.; Hess, B.; Van der Spoel, D. GROMACS 3.0: A package for molecular simulation and trajectory analysis. *J. Mol. Model.*, **2001**, *7*, 306-317.
[120] Gonzalez-Melchor, M.; Bresme, F.; Alejandre, J. Molecular dynamics simulations of the surface tension of ionic liquids. *J. Chem. Phys.*, **2005**, *122*, 104710-104718.
[121] Pensado, A.S.; Gomes, M.F.C.; Canongia Lopes, J.N.; Malfreyt, P.; Padua, A.A.H. Effect of alkyl chain length and hydroxyl group functionalization on the surface properties of imidazolium ionic liquids. *Phys. Chem. Chem. Phys.*, **2011**, *13*, 13518-13526.
[122] Chaban, V. Polarizability versus mobility: atomistic force field for ionic liquids. *Phys. Chem. Chem. Phys.*, **2011**, *13*, 16055-16062.
[123] Canongia Lopes, J.N.; Padua, A.A.H. Molecular force field for ionic liquids III: Imidazolium, pyridinium, and phosphonium cations; Chloride, bromide, and dicyanamide anions. *J. Phys. Chem. B*, **2006**, *110*, 19586-19592.
[124] Shimizu, K.; Almantariotis, D.; Gomes, M.F.C.; Padua, A.A.H.; Lopes, J.N.C. Molecular force field for ionic liquids v: hydroxyethylimidazolium, dimethoxy-2-methylimidazolium, and fluoroalkylimidazolium cations and bis(fluorosulfonyl)amide, perfluoroalkanesulfonylamide, and fluoroalkylfluorophosphate anions. *J. Phys. Chem. B*, **2010**, *114*, 3592-3600.
[125] Chaban, V.V.; Voroshylova, I.V.; Kalugin, O.N. A new force field model for the simulation of transport properties of imidazolium-based ionic liquids. *Phys. Chem. Chem. Phys.*, **2011**, *13*, 7910-7920.
[126] Schroeder, C.; Steinhauser, O. Simulating polarizable molecular ionic liquids with Drude oscillators. *J. Chem. Phys.*, **2010**, *133*, 154511-154513.
[127] Dommert, F.; Schmidt, J.; Krekeler, C.; Zhao, Y.Y.; Berger, R.; Delle Site, L.; Holm, C. Towards multiscale modeling of ionic liquids: From electronic structure to bulk properties. *J. Mol. Liq.*, **2010**, *152*, 2-8.
[128] Reed, A.E.; Weinstock, R.B.; Weinhold, F. Natural-population analysis. *J. Chem. Phys.*, **1985**, *83*, 735-746.
[129] Jacquemin, J.; Husson, P.; Mayer, V.; Cibulka, I. High-pressure volumetric properties of imidazolium-based ionic liquids: Effect of the anion. *J. Chem. Eng. Data*, **2007**, *52*, 2204-2211.
[130] Domanska, U.; Laskowska, M. Temperature and composition dependence of the density and viscosity of binary mixtures of {1-butyl-3-methylimidazolium thiocyanate+1-alcohols}. *J. Chem. Eng. Data*, **2009**, *54*, 2113-2119.
[131] Suarez, P.A.Z.; Einloft, S.; Dullius, J.E.L.; De Souza, R.F.; Dupont, J. Synthesis and physical-chemical properties of ionic liquids based on 1-n-butyl-3-methylimidazolium cation. *J. Chim. Phys. Phys.- Chim. Biol.*, **1998**, *95*, 1626-1639.
[132] Krummen, M.; Wasserscheid, P.; and Gmehling, J. Measurement of activity coefficients at infinite dilution in ionic liquids using the dilutor technique. *J. Chem. Eng. Data*, **2002**, *47*, 1411-1417.
[133] Kandil, M.E.; Marsh, K.N.; Goodwin, A.R.H.; Measurement of the viscosity, density, and electrical conductivity of 1-hexyl-3-methylimidazolium bis(trifluorosulfonyl)imide at temperatures between (288 and 433) K and pressures below 50 MPa. *J. Chem. Eng. Data*, **2007**, *52*, 2382-2387.
[134] Soriano, A.N.; Doma Jr, B.T.; Li, M.-H. Measurements of the density and refractive index for 1-n-butyl-3-methylimidazolium-based ionic liquids. *J. Chem. Thermodyn.*, **2009**, *41*, 301-307.
[135] Shiflett, M.B.; Kasprzak, D.J.; Junk, C.P.; Yokozeki, A. Phase behavior of {carbon dioxide + [bmim][Ac]} mixtures. *J. Chem. Thermodynam.*, **2008**, *40*, 25-31.
[136] Domańska, U.; Mazurowska, L. Solubility of 1,3-dialkylimidazolium chloride or hexafluorophosphate or methylsulfonate in organic solvents: Effect of the anions on solubility. *Fluid Phase Equilib.*, **2004**, *221*, 73-82.

[137] Dibrov, S.M.; Kochi, J.K. Crystallographic view of fluidic structures for room-temperature ionic liquids: 1-butyl-3-methylimidazolium hexafluorophosphate. *Acta Crystallograph. Section C-Crystal Struct. Commun.*, **2006**, *62*, O19-O21.

[138] Reichert, W.M.; Holbrey, J.D.; Swatloski, R.P.; Gutowski, K.E.; Visser, A.E.; Nieuwenhuyzen, M.; Seddon, K.R.; Rogers, R.D. Solid-stute analysis of low-melting 1,3-dialkylimidazolium hexafluorophosphate salts (ionic liquids) by combined x-ray crystallographic and computational analyses. *Cryst. Growth Design*, **2007**, *7*, 1106-1114.

[139] Deyko, A.; Lovelock, K.R.J.; Corfield, J.A.; Taylor, A.W.; Gooden, P.N.; Villar-Garcia, I.J.; Licence, P.; Jones, R.G.; Krasovskiy, V.G.; Chernikova, E.A.; Kustov, L.M. Measuring and predicting $\Delta_{vap}H_{298}$ values of ionic liquids. *Phys. Chem. Chem. Phys.*, **2009**, *11*, 8544-8555.

[140] Emelyanenko, V.N.; Verevkin, S.P.; Heintz, A. Pyridinium based ionic liquids. N-Butyl-3-methyl-pyridinium dicyanoamide: Thermochemical measurement and first-principles calculations. *Thermochim. Acta*, **2011**, *514*, 28-31.

[141] Deyko, A.; Hessey, S.G.; Licence, P.; Chernikova, E.A.; Krasovskiy, V.G.; Kustov, L.M.; Jones, R.G. The enthalpies of vaporisation of ionic liquids: new measurements and predictions. *Phys. Chem. Chem. Phys.*, **2012**, *14*, 3181-3193.

[142] Tokuda, H.; Hayamizu, K.; Ishii, K.; Susan, M.; Watanabe, M.; Physicochemical properties and structures of room temperature ionic liquids. 1. Variation of anionic species. *J. Phys. Chem. B*, **2004**, *108*, 16593-16600.

[143] Tokuda, H.; Tsuzuki, S.; Susan, M.; Hayamizu, K.; Watanabe, M.; How ionic are room-temperature ionic liquids? An indicator of the physicochemical properties. *J. Phys. Chem. B*, **2006**, *110*, 19593-19600.

[144] Tokuda, H.; Hayamizu, K.; Ishii, K.; Susan, M.; Watanabe, M. Physicochemical properties and structures of room temperature ionic liquids. 2. Variation of alkyl chain length in imidazolium cation. *J. Phys. Chem. B*, **2005**, *109*, 6103-6110.

[145] Tokuda, H.; Ishii, K.; Susan, M.; Tsuzuki, S.; Hayamizu, K.; Watanabe, M. Physicochemical properties and structures of room-temperature ionic liquids. 3. Variation of cationic structures. *J. Phys. Chem. B*, **2006**, *110*, 2833-2839.

Received: July 18, 2012 Revised: December 01, 2012 Accepted: January 18, 2013